

**YFS2 - THE SECOND ORDER MONTE CARLO  
FOR FERMION PAIR PRODUCTION AT LEP/SLC  
WITH THE INITIAL STATE RADIATION OF  
TWO HARD AND MULTIPLE SOFT PHOTONS**

STANISLAW JADACH

*Institute of Physics, Jagellonian University  
30-059 Kraków, ul. Reymonta 4, Poland*

and

B. F. L. WARD

*Department of Physics and Astronomy,  
The University of Tennessee, Knoxville, Tennessee 37996-1200, U.S.A.*

and

*Stanford Linear Accelerator Center,  
Stanford University, Stanford, California 94309, U.S.A.*

**ABSTRACT**

A Monte Carlo program simulating fermion pair production is presented. It features a multiphoton bremsstrahlung out of the initial state beams. The contributions from soft photons are summed rigorously up to an infinite order using the Yennie-Frautschi-Suura method while the contributions from up to two hard photons are also properly treated. Four momenta of all soft and hard photons are explicitly generated and the total energy momentum conservation is exactly obeyed. The program is primarily aimed for LEP/SLC type experiments and will be helpful in the precise measurements of the  $Z^0$  mass and width, the basic parameters in precision tests of standard electroweak theory. It can also be used far away from the  $Z^0$  resonance as well. From the point of view of the QED it provides the total cross section with precision 0.1% near  $Z^0$  and 0.5% away from  $Z^0$  resonance. With some restriction it can provide predictions for various asymmetries.

*(To be submitted to Computer Physics Communications)*

## PROGRAM SUMMARY

*Title of the program:* YFS2.02

*Computer:* IBM; *Installation:* IBM 3081/3090/3033

*Operating system:* CERNVM, SLACVM, UTKVM1

*Programing language used:* FORTRAN 77

*High speed storage required:* 100000 words

*No. of bits in a word:* 32

*Peripherals used:* Line printer

*No. of cards in combined program and test deck:* 1339

*Keywords:* Radiative corrections, initial state bremsstrahlung, Monte Carlo simulation, Quantum Electrodynamics, exponentiation, multiphoton emission,  $Z^0$  boson,  $e^+e^-$  annihilation, electroweak theory.

### *Nature of physical problem:*

High statistics data samples will be available soon in LEP and SLC experiments allowing for a precise measurements of the  $Z^0$  mass, width and various asymmetries. Since initial state QED bremsstrahlung distorts the shape of the  $Z^0$  resonance very strongly it will not be possible to make any statement about the agreement of these data with the standard electroweak model before one is able to calculate all these effects very precisely. The above QED effects depend usually on the experimental acceptance and selection criteria and it is therefore practically impossible to calculate them analytically. It is already known that in order to reach a sufficient precision level one has to sum up contributions from multiple soft photons and from up to two hard photons. In particular any program of the class presented in ref. [1] is not sufficiently precise. A number of analytical exact and approximate calculations exist for the total cross section [2,3]. They are very instructive but they cannot help in removing detector acceptance from the data and/or provide the integrated cross section in the presence of the realistic, complicated set of cut-offs.

### *Method of solution:*

The Monte Carlo event generator is the well known answer to the above problems. Any given experimental acceptance and cut-offs may be introduced easily by rejecting some part of the generated events. The main technical problem in the construction of the Monte Carlo event generator with multiple soft and hard photons is related to a necessity of generating photon momenta within a multibody Lorentz invariant phase space with the simultaneous

importance sampling for strong singularities due to the bremsstrahlung matrix element and  $Z^0$  resonance. An elegant solution of this problem, being an extension of the methods described in refs. [4], is presented in this work.

*Restrictions on the complexity of the problem:*

Outgoing fermion  $f$  may be any lepton or quark except of  $f = e^-, \nu_e$ . The program is best suited for calculating the total cross section and the spin asymmetry with respect to beam polarization and also for all sorts of the detector acceptance studies. Pure electroweak corrections are not included, but we provide a detailed explanation of how to do it. Due to omission of the final state bremsstrahlung and its interference with the initial state bremsstrahlung this program cannot be used for calculation of the final state polarization asymmetry ( $\tau$  pair production) and some care is necessary in the case of calculation of the forward backward asymmetry.

*Typical running time:*

- CPU time for one event depends on center of mass energy and infrared cut-off. Typically, at the  $Z^0$  position generating 1000 events costs 9 CPU seconds and off  $Z^0$  resonance about 18 CPU seconds on the IBM 3081.

*References:*

- [1] F. A. Berends, R. Kleiss and S. Jadach, Comp. Phys. Commun. **29**, 185 (1983).
- [2] F. A. Berends and W. L. Van Neerven and G. J. H. Burgers, Nucl. Phys. **B297** (1988) 249.
- [3] E.A. Kuraev and V.S. Fadin, Sov. J. Nucl. Phys. **41** (1985) 466;  
G. Altarelli and G. Martinelli, in "Physics at LEP", ed. J. Ellis and R. Peccei, CERN Report 86-02 vol. 1 p. 47.
- [4] S. Jadach, "Yennie-Frautschi-Suura soft photons in the Monte Carlo generators", preprint of Max-Planck-Institut, München, MPI-PAE/PTh 6/87 (1987)  
and S. Jadach and B. F. L. Ward, SLAC-PUB-4543 (1988), Phys. Rev. **D38**, (1988), 2897.

## 1. Introduction

In the recent years an impressive evidence has been accumulated in a variety of experiments, including direct observation of  $Z^0$  and  $W^\pm$  bosons in  $p\bar{p}$  collider, in support of the standard electroweak model [1]. A new qualitative step in its experimental verification will take place soon with the advent of the LEP and SLC  $e^+e^-$  colliders where high statistics data near the  $Z^0$  resonance will become available.

The first and simplest measurement of the total cross section will provide new precise values of the  $Z^0$  mass and width. In the next step the laborious measurements of various asymmetries will provide detailed new information on the  $Z^0$  couplings to leptons and quarks. There is a well known problem, however, with the measurement of the  $Z^0$  mass, width and peak cross section which is due to the initial state QED bremsstrahlung. The frequent emission of the (usually soft) photons out of the initial beams distorts strongly the Breit-Wigner  $Z^0$  resonance shape lowering the peak cross section by  $-26\%$  and shifting the peak position by about  $+110\text{MeV}$ . In the radiative tail above the  $Z^0$  position the QED corrections are even larger, of order  $100\%$ . The emission of additional photons affects not only the total cross section but also topology of the events giving rise to nonzero acollinearity and acoplanarity angles for final fermions and to nonzero transverse momentum of the final fermion pair as a whole.

Since the above QED effects do not carry any new physical information and may only obscure the measurements of new interesting phenomena, it is therefore highly desirable to calculate and to eliminate them from the data at the precision level of a factor of  $2 - 3$  better than the best anticipated experimental error. This means that the QED initial state bremsstrahlung effects in the total cross section should be under control below  $0.5\%$ . From the various non-Monte-Carlo (analytical) calculations [2-4] it is known that in order to reach a sufficient precision level it is necessary to include QED initial state corrections from up to two real/virtual photons and it is strongly recommended to sum up the contribution from the infinite number of soft photons<sup>(1)</sup>. The serious drawback of these calculations is that they feature very simple kinematical limits on the photons, as in ref. [2], or they have unspecified (and non-conserved) transverse photon momenta, as in. refs. [3,4]. In the real experiment the combined effect of detector acceptance and

---

(1) See also ref. [5] for a summary review of these calculations.

of the selection criteria cannot be cast into a simple analytical form such that one may attempt to integrate the cross section analytically. At LEP/SLC experiments a Monte Carlo event generator will be for this purpose *indispensable*, similarly as it was in the former PETRA/PEP experiments. Presently, the only published and documented Monte Carlo event generator for the fermion pair production process at LEP/SLC energies is that of ref. [6]. It includes single photon emission only, provides the total cross section with low precision and lacks kinematical effects due to emission of the second real photon. It is definitely insufficient for LEP/SLC experiments.

One of the main lessons from refs. [2,3,5] is that due to strong variation of the lowest order cross section near the  $Z^0$  resonance one has, first of all, to sum up the contributions from multiple soft photons. The contribution from hard photon(s) really matters far away from the  $Z^0$  resonance, especially in its radiative tail. The Monte Carlo event generator presented in this paper is based on the rigorous resummation of soft photon contributions according to the Yennie-Frautschi-Suura (YFS) method [7]. The first, still rather simple, version of the Monte Carlo algorithm used in this work was presented in ref. [8]. Some numerical results obtained from the first unpublished version of this program were presented in ref. [9]. A supplementary discussion on the underlying ideas exploited in this work the reader may find in refs. [10].

Is the strategy of the present work for calculating the higher order QED effects to concentrate first on the proper soft photon summation the only possible one? Of course it is not. Let us comment on the other options and try to explain very briefly how do they compare with the ours. It is known that much of the effects due to the initial state radiation can be qualitatively explained and calculated in a simplified picture where both  $e^\pm$  beams fragment collinearly into photons and another  $e^\pm$  beam such that at the moment of  $e^-e^+$  annihilation the total center of the mass energy is reduced and the annihilation cross section changed accordingly, see refs. [3-5]. This type of the calculation is physically very appealing and it gives a rather quick answer for the total cross section near the  $Z^0$  with about 1-2% precision. One may even construct a Monte-Carlo event generator in which photons are emitted with zero  $p_T$  with respect to the  $e^\pm$  beams. After a quick start, one faces the problems, however. In order to improve on the precision of the result the beam fragmentation distributions have to be modified by hand in the soft photon limit. Generally, in this approach in order to improve further on the precision one has to go beyond the leading-log approximation. This can be done for the *inclusive* quantities like the total cross section [2] but unfortunately there is no known way (apart from guesses) to proceed systematically, beyond the leading-log, with the *exclusive* distributions necessary

for a Monte Carlo program event generator. The attempts of constructing Monte Carlo event generators in this spirit suffer from a large degree of arbitrariness and a lack of a good estimate of the actual precision of the result. In fact the only procedure for estimating the final error is to compare the results from various different, ad-hoc, procedures.

The other possible, conservative, strategy would be to make a second order Monte Carlo event generator, without any “exponentiation”, following closely the work of ref. [6]. (The corresponding analytical exact second order calculation for the total cross section is already done, [2].) This approach seems, however, to be not very attractive. The first order Monte Carlo of ref. [6] is plagued with the positivity problem of the soft photon cross section: The integrated cross section with no photons above the energy cut-off  $E_{max}^\gamma$  is roughly proportional to  $1 - \delta_s$  where

$$\delta_s = 2 \left( \frac{\alpha}{\pi} \right) \ln \left( \frac{s}{m_e^2} \right) \ln \left( \frac{\sqrt{s}}{2E_{max}^\gamma} \right) \quad (1.1)$$

includes a large Sudakov-type double-logarithm and therefore  $1 - \delta_s$  may easily become negative – a disaster for the Monte-Carlo. In the second order situation gets improved because this particular cross section becomes proportional to the factor  $1 - \delta_s + \frac{1}{2}\delta_s^2$  which does not get negative ( but may get excessively positive instead). The positivity problem returns, however, in the previous bad form, in the case of one photon above and up to one real/virtual photon below  $E_{max}^\gamma$  (the corresponding cross section is again proportional to  $1 - \delta_s$ ). Our scheme is superior to the above solution because the summation over the infrared/soft photon contributions necessarily involves a summation of the Sudakov double-logarithmic contribution to an infinite order at the very beginning and the positivity of the differential cross section is assured automatically. Compared with the leading/next-to-leading log scheme our approach does not offer a quick start because one has to invest in the development of the new nontrivial type of the Monte-Carlo generator, but once it is done, the inclusion of the second order corrections, and of the higher ones if necessary, is relatively easy and the remaining series in the number of noninfrared/hard photons is rapidly convergent (no double logs). The two above approaches are complementary and if, at some point, the problems with the proper definition of the exclusive spectra in the next-to-leading log approach are solved, then its comparison with our scheme would be a very interesting exercise.

How do we estimate the overall precision in our approach? The soft photon corrections are summed up to an infinite order, rigorously from the point of view of perturbative QED [7], and the noninfrared/hard photon contributions are added in the scattering matrix

element one by one, i.e., order by order. The basic method is to compare the results from the first and second order calculations.<sup>(2)</sup> Another possibility is to compare two second order results, the usual one with the series over the noninfrared/hard photons including three terms (up to two hard photons) and another truncated to two terms only. The precision of the calculated cross section is deduced from the difference between the two results. The following estimate of the precision is obtained from these two methods: in the region up to  $3\text{GeV}$  away from the  $Z^0$  position the precision is better than 0.1% and far away from the  $Z^0$  it is better than 0.5%.

The presented program provides not only information on the total cross section but also on the topology of the experimental events. Let us first explain what the title statement about applicability of our program to two hard and multiple soft photons means. The program in fact is generating events with three and more hard photons as well. The restriction to two hard photons comes only from the fact that for three and more hard photons the matrix element will be not correct<sup>(3)</sup>. There are two ways to proceed with these multi-hard events, either let them in the sample, knowing that they contribute negligibly ( $\leq 0.01\%$ ) to the total cross section, or to reject them with the experimentally feasible cut-offs. Near the top of the  $Z^0$  peak the rapidly falling cross section acts as an effective cut-off on the hard photon emission.<sup>(4)</sup> If the experimental cut-offs are loose then the dependence of the total cross section and of other observables on cut-offs will be rather weak. Nevertheless the resolution in the typical LEP/SLC experiments will be very sharp and the effects due to emission of multiple photons will be clearly visible in many distributions, for example in the acollinearity/acoplanarity distribution of the outgoing fermions or in the total longitudinal/transverse momentum distribution of the fermion pair. The present program offers a definite and precise QED prediction for these distributions and they may be very useful in calibrating the detector and/or testing the QED as well. Some of these distributions depend also on photons emitted from the final state which are not yet included in the present version of the program. In this case we recommend the user to employ the unpublished but widely available program KORALZ [11] in which the present program is supplemented with the final state bremsstrahlung in an approximate way. This is a temporary solution and the real one will come with the next version of the present program. We would like also to note that the first version of the multiphoton event generator

---

(2) In fact, as is explained in Section 3, the contribution to the differential cross section from the second noninfrared/hard photon is added in the leading-logarithm approximation. Some of next-to-leading corrections are also included. This is enough for the precision level claimed in this paper.

(3) It will be not dramatically wrong, factor two at most.

(4) For the initial state emission only.

with the Yennie-Frautschi-Suura soft photon summation exists for the low angle Bhabha scattering [12]. It is aimed primarily at the luminosity type measurements.

The layout of the paper is the following: In Section 2 we describe the Monte Carlo algorithm; in Section 3 we write down and explain in detail the QED differential cross section used in the event generation; in Section 4 the structure of the program is explained and the important subprograms and variables are listed; in Section 5 we describe how to use the program, what sort of input is required and where to find the interesting output; finally, in Section 6 we give the examples on the numerical results concentrating on the precision of the total cross section and we provide a further information on the output from the program. Short conclusions are given in Section 7.

The question of the area of applicability of the program is discussed in Sections 5 and 6. We conclude that the program in the present version is well suited for the total cross section<sup>(5)</sup> and for the polarization asymmetry with respect to the initial beam. With some restrictions it can be used for the charge asymmetry at the top of the  $Z^0$ . It is not helpful for calculating the final state polarization asymmetry, unless it is taken as a part of KORALZ [11]. The present program can be easily interfaced with any reasonable program for pure electroweak corrections and we instruct the user at the end of Section 5 in how to do it in practice. In Section 6 we also present an example of numerical results from the Monte Carlo calculation based on the renormalization group improvement – another possible application of the presented program.

## 2. The Monte Carlo algorithm

Let us start with a formula for the total cross section which includes phase space integrals in a form ready for the Monte Carlo integration. The relation to the standard Yennie-Frautschi-Suura notation [7], used also in many other papers on the exponentiation, see for instance refs. [13,14], can be found in the Appendix A. The differential cross section for the process

$$e^-(p_1) + e^+(p_2) \rightarrow f(q_1) + \bar{f}(q_2) + \gamma(k_1) + \dots + \gamma(k_n) \quad (2.1)$$

is summed over the photon multiplicity  $n$  and integrated over the Lorentz invariant phase

---

(5) For the integrated cross section the influence of the final state bremsstrahlung is negligible, provided the cut-offs are mild (or absent), but it becomes quickly quite important in the presence of any stronger kinematical cut-offs.



space in the following way

$$\begin{aligned} \sigma = & \sum_{n=0}^{\infty} \frac{1}{n!} \int \frac{d^3 q_1}{q_1^0} \frac{d^3 q_2}{q_2^0} \left( \prod_{i=1}^n \frac{d^3 k_i}{k_i^0} \tilde{S}(p_1, p_2, k_i) \right) \delta^4(p_1 + p_2 - q_1 - q_2 - \sum_{i=1}^n k_i) \Theta_{\epsilon}^{cm} \\ & \exp \left( 2\alpha B + \int \frac{d^3 k}{k^0} \tilde{S}(p_1, p_2, k) (1 - \theta_{\epsilon}^{cm}(k)) \right) \frac{2}{\beta_f} \left( \tilde{\beta}_0(\mathcal{R}p_1, \mathcal{R}p_2, \mathcal{R}q_1, \mathcal{R}q_2) \right. \\ & \left. + \sum_{l=1}^n \frac{\tilde{\beta}_1(\mathcal{R}p_1, \mathcal{R}p_2, \mathcal{R}q_1, \mathcal{R}q_2, k_l)}{\tilde{S}(k_l)} + \sum_{\substack{l,j=1 \\ l \neq j}}^n \frac{\tilde{\beta}_2(\mathcal{R}p_1, \mathcal{R}p_2, \mathcal{R}q_1, \mathcal{R}q_2, k_l, k_j)}{\tilde{S}(k_l) \tilde{S}(k_j)} \right). \end{aligned} \quad (2.2)$$

Let us explain the main ingredients in the above expression.

(i) The infrared singularity in the factors

$$\tilde{S}(p_1, p_2, k) = -\frac{\alpha}{4\pi^2} \left( \frac{p_1}{p_1 k} - \frac{p_2}{p_2 k} \right)^2 = \frac{\alpha}{4\pi^2} \left( \frac{2p_1 p_2}{(p_1 k)(p_2 k)} - \frac{m_e^2}{(p_1 k)^2} - \frac{m_e^2}{(p_2 k)^2} \right) \quad (2.3)$$

is excluded from the integration domain by means of the conventional energy cut-off in the center of mass system. This is done with the help of

$$\Theta_{\epsilon}^{cm} = \prod_{i=1}^n \theta \left( \frac{2k_i^0}{\sqrt{s}} - \epsilon \right) \quad (2.4)$$

which is equal zero if an energy of any of the photons falls below  $\epsilon\sqrt{s}/2$ ,  $s = 2p_1 \cdot p_2$  and we require  $\epsilon \ll 1$ .

(ii) The integral includes hard photons all over the complete phase space.

(iii) The explicit dependence of the integrated cross section in eq. (2.2) on the infrared cut-off  $\epsilon$ , coming from the lower integration limits, is in fact completely canceled by the Yennie-Frautschi-Suura [7] form-factor

$$\begin{aligned} F_{\text{YFS}}(p_1, p_2, \epsilon) &= \exp \left( 2\alpha \text{Re} B + \int \frac{d^3 k}{k^0} \tilde{S}(p_1, p_2, k) \left( 1 - \theta \left( k^0 - \frac{2\epsilon}{\sqrt{s}} \right) \right) \right) \\ &= \exp \left( 2\frac{\alpha}{\pi} \left( \left[ \ln \frac{s}{m_e^2} - 1 \right] \ln \epsilon + \frac{1}{2} \ln \frac{s}{m_e^2} - 1 + \frac{\pi^2}{3} \right) \right), \end{aligned} \quad (2.5)$$

where the approximation  $m_e^2/s \ll 1$  was used, see ref. [9] and Appendix A for definition of  $2\alpha B$  and for other details. Neither the total cross section nor any other measurable quantity depends on  $\epsilon$ . It plays only a role of a dummy parameter introduced to limit the multiplicity of very soft photons for the purpose of the numerical M. C. integration and it

may be set arbitrarily low.

(iv) The functions  $\tilde{\beta}_{0,1,2}$  are infrared finite and are calculated perturbatively order by order. In our case one needs the second order – two loop – double bremsstrahlung matrix elements to extract them. The relevant formal definitions of  $\tilde{\beta}$ 's are given in refs. [10] and the first order formulae for  $\tilde{\beta}_{0,1}$  can be found in ref. [9]. The complete definitions of  $\tilde{\beta}$ 's used in this program are listed in Section 3. The normalization factor  $2/\beta_f = 2(1 - m_f^2/(q_1 + q_2)^2)^{-1/2}$  was adjusted such that the lowest order  $\tilde{\beta}_0$  is simply

$$\tilde{\beta}_0^{(0)}(p_i, q_i) \equiv \frac{d\sigma_{\text{Born}}}{d\Omega}(\theta, s).$$

(v) The meaning of the  $\mathcal{R}p_i$  and  $\mathcal{R}q_i$  is the following. Strictly speaking  $\tilde{\beta}_{0,1,2}$  are defined within the corresponding 2, 3 and 4 body phase space and if for a particular photon multiplicity in the formula (2.2) there are some additional photons then the proper mapping  $p_i \rightarrow \mathcal{R}p_i$  and  $q_i \rightarrow \mathcal{R}q_i$  in the arguments of  $\tilde{\beta}_{0,1,2}$  has to be performed. In other words one has to require [7]

$$\begin{aligned} \mathcal{R}p_1 + \mathcal{R}p_2 &= \mathcal{R}q_1 + \mathcal{R}q_2 \quad \text{for} \quad \tilde{\beta}_0(\mathcal{R}p_1, \mathcal{R}p_2, \mathcal{R}q_1, \mathcal{R}q_2), \\ \mathcal{R}p_1 + \mathcal{R}p_2 &= \mathcal{R}q_1 + \mathcal{R}q_2 + k_l \quad \text{for} \quad \tilde{\beta}_1(\mathcal{R}p_1, \mathcal{R}p_2, \mathcal{R}q_1, \mathcal{R}q_2, k_l) \quad \text{and} \\ \mathcal{R}p_1 + \mathcal{R}p_2 &= \mathcal{R}q_1 + \mathcal{R}q_2 + k_l + k_j \quad \text{for} \quad \tilde{\beta}_2(\mathcal{R}p_1, \mathcal{R}p_2, \mathcal{R}q_1, \mathcal{R}q_2, k_l, k_j). \end{aligned} \tag{2.6}$$

As we see, each of the above mappings is the projection of the phase space point onto an edge of the phase space, where the edge by itself is a less-dimensional phase space. This procedure is related to the fact that in the YFS scheme of ref. [7] the infrared singular factors  $\tilde{S}$  are subtracted and the residues, equal to  $\tilde{\beta}$ 's, are taken at the singularity position ( $k^0 = 0$ ). The  $\mathcal{R}$  procedure concerns only the arguments of  $\tilde{\beta}_i$  and does not disturb the phase space integral nor the four-momentum conservation. The reduction procedure  $\mathcal{R}$  *may* depend on the momenta of all fermions but *may not* depend on the momenta of the individual photons. This requirement is crucial for the cancellation of the infrared divergences in eq. (2.2). A definition of the  $\mathcal{R}$  procedure for  $\tilde{\beta}_0$  will be given later on in this Section and a detailed definition of the  $\mathcal{R}$  operation for all  $\tilde{\beta}$ 's is included in Section 3.

We shall now introduce the reader to the method of generating Monte Carlo events. The procedure of constructing our Monte Carlo algorithm is generally the following: we shall gradually simplify the integrand and the phase space limits such that at the end we obtain a simple distribution which can be easily generated with help of the uniform random

numbers. All these modifications have to be corrected for by the appropriate reweighting and rejecting the events which were generated according to the simplified distribution. At the end of this section we shall summarize on all weights which have been introduced in the course of the simplifications. The exact integrated cross section is calculable numerically using the average weights from the Monte Carlo run and may be obtained with an arbitrary precision, simply by increasing the number of generated events.

In the first place we drop out higher  $\tilde{\beta}$ 's

$$\tilde{\beta}_1 \longrightarrow 0, \quad \tilde{\beta}_2 \longrightarrow 0. \quad (2.7)$$

As we shall see later on, the effects of  $\tilde{\beta}_{1,2}$  are small and, therefore, they can be easily reinstalled in the late stage of the Monte Carlo by the rejection procedure.

A next replacement

$$\tilde{\beta}_0 \longrightarrow b_0 = \frac{1}{4\pi} \sigma_{\text{Born}}((q_1 + q_2)^2) \quad (2.8)$$

is more meaningful and it should be understood as follows. First of all, since we are dealing with the resonance production we must take into account the effective shift of the center of the mass energy [7]

$$s \longrightarrow s' = (q_1 + q_2)^2 \quad (2.9)$$

in the matrix element, already in  $\tilde{\beta}_0$ . This is done by requiring that the reduction procedure (n.b. for all  $\tilde{\beta}$ 's) fulfills the condition

$$(q_1 + q_2)^2 = (\mathcal{R}q_1 + \mathcal{R}q_2)^2. \quad (2.10)$$

The  $\mathcal{R}$  procedure for  $\tilde{\beta}_0$  goes as follows. Starting from the laboratory system (center of the mass system for the initial beams) with the third axis pointing along  $e^-$  we make a  $z$ -boost such that  $q_1^3 + q_2^3 = 0$  and then another boost along the remaining transverse part of  $\vec{q}_1 + \vec{q}_2$  to a rest frame of  $q_1 + q_2$ . In this frame we assign the resulting  $q_i$  as  $\mathcal{R}q_i$  and the four-momenta  $\mathcal{R}p_i$  are simply constructed as  $p_1 = (\sqrt{s'}/2, 0, 0, p_z)$ ,  $p_2 = (\sqrt{s'}/2, 0, 0, -p_z)$  where  $p_z = \sqrt{s'/4 - m_e^2}$  <sup>(6)</sup>. Obviously, this construction fulfills conditions (2.6) and

---

(6) This procedure coincides well with the leading-log/collinear approximation prescription which says: take the Born differential cross section at the reduced center of the mass system with the  $z$ -axis pointing in this frame roughly in the direction of the beam momenta.

(2.10). In fact, neglecting the virtual correction, one may well approximate [9]

$$\tilde{\beta}_0(\mathcal{R}p_1, \mathcal{R}p_2, \mathcal{R}q_1 \mathcal{R}q_2) \simeq \frac{d\sigma_{\text{Born}}}{d\Omega}(s', \theta_q),$$

where  $\theta_q$  is an angle between  $\mathcal{R}p_1$  and  $\mathcal{R}q_1$ . In the eq. (2.8) we go on however one step further and we also neglect the angular dependence on  $\theta_q$ . This is done for the purpose of the modularity of the program. From now on we have only to worry about the squared bremsstrahlung matrix element factor  $\prod_i \tilde{S}(k_i)$  and about the resonance curve embodied in the  $\sigma_{\text{Born}}(s')$ . The whole complicated details about the higher order real and virtual corrections are added in the late stage of the Monte Carlo by rejection and are functionally very well separated from the rest of the program.

The net distribution which now remains for discussion is the following

$$\sigma' = F_{\text{YFS}}(p_1, p_2, \epsilon) \sum_{n=0}^{\infty} \frac{1}{n!} \int \prod_{i=1}^n \frac{d^3 k_i}{k_i^0} \tilde{S}(p_1, p_2, k_i) \Theta_{\epsilon}^{cm} \int \frac{d\Omega_q}{4\pi} \sigma_{\text{Born}}(s'). \quad (2.11)$$

The  $Z^0$  resonance is so sharp that we have to arrange the phase space integration and the Monte Carlo algorithm in a special way; the variable  $s' = (q_1 + q_2)^2$  must be generated first with an appropriate importance sampling. Let us introduce a new variable

$$v = 1 - \frac{s'}{s} = \frac{2KP - K^2}{P^2}, \quad P = p_1 + p_2, \quad K = \sum_{i=1}^n k_i \quad (2.12)$$

as a first variable in our integral

$$\sigma' = F_{\text{YFS}}(p_1, p_2, \epsilon) \int_{\epsilon}^{v_{\max}} dv \int \frac{d\Omega_q}{4\pi} \sigma_{\text{Born}}(s(1-v)) \sum_{n=0}^{\infty} \frac{1}{n!} \int \prod_{i=1}^n \frac{d^3 k_i}{k_i^0} \tilde{S}(k_i) \Theta_{\epsilon}^{cm} \delta\left(v - \frac{2KP - K^2}{P^2}\right). \quad (2.13)$$

The condition  $v \geq \epsilon$  is induced by  $\Theta_{\epsilon}^{cm}$ , because due to  $\epsilon \ll 1$  the term  $K^2$  in (2.12) can be safely neglected. The upper limit  $v_{\max}$  on the photon phase space is in principle arbitrary but it must obviously obey  $v_{\max} < 1 - 4m_f^2/s$ .

Now comes the main point in the Monte Carlo algorithm: for a fixed value of the variable  $v$  we have to generate four momenta of  $n$  photons according to a distribution  $\prod_{i=1}^n \tilde{S}(k_i)$  with the constraint of eq. (2.12). The solution of the problem which shall

be shown quite in a detail in the following is quite similar to that presented in ref. [8], see also ref. [15]. It consists roughly in replacing the constraint (2.12) by a simpler one. Photon momenta are generated according to the simplified constraint and the original one is recovered later on by rescaling the four momenta of all photons accordingly.

The essential preparatory step in the above procedure is the introduction of the new integration variables for the photon momenta which we shall illustrate on the integral

$$\sigma'_n(v) = F_{\text{YFS}} \sigma_{\text{Born}}(s') \int \prod_{i=1}^n \frac{d^3 k_i}{k_i^0} \hat{S}(k_i) \delta\left(v - \frac{2KP - K^2}{P^2}\right) \prod_{i=1}^{n-1} \theta(k_{i+1}^0 - k_i^0) \theta(k_n^0 - \frac{\sqrt{s}}{2}\epsilon). \quad (2.14)$$

In the above we have introduced an ordering of the photon energies at the expense of the  $1/n!$  factor and, as a result, the function  $\Theta_\epsilon^{\text{cm}}$  was replaced by the single  $\theta$  function depending on the smallest energy  $k_n^0$ . Let us introduce now an auxiliary variable  $\lambda$  and a new delta function representing the simplified constraint

$$\sigma'_n(v) = F_{\text{YFS}} \sigma_{\text{Born}}(s') \int d\lambda \int \prod_{i=1}^n \frac{d^3 k_i}{k_i^0} \hat{S}(k_i) \delta\left(\lambda - \frac{2k_1 P}{vP^2}\right) \delta\left(v - \frac{2KP - K^2}{P^2}\right) \prod_{i=1}^{n-1} \theta(k_{i+1}^0 - k_i^0) \theta(k_n^0 - \frac{\sqrt{s}}{2}\epsilon). \quad (2.15)$$

Then, we rescale all photon four momenta  $k_i = \lambda \bar{k}_i$  and, next, eliminate the old delta function by integrating over  $\lambda$ . In the resulting integral

$$\sigma'_n(v) = F_{\text{YFS}} \sigma_{\text{Born}}(s') \int \prod_{i=1}^n \frac{d^3 \bar{k}_i}{\bar{k}_i^0} \hat{S}(\bar{k}_i) \delta\left(\frac{2\bar{k}_1^0}{\sqrt{s}} - v\right) \theta(\bar{k}_1^0 - \bar{k}_2^0) \theta(\bar{k}_2^0 - \bar{k}_3^0) \dots \theta(\bar{k}_{n-1}^0 - \bar{k}_n^0) \theta(\bar{k}_n^0 \lambda_0(\bar{K}, v) - \frac{\sqrt{s}}{2}\epsilon) \mathcal{J}(\bar{K}, v) \quad (2.16)$$

the new constraints simply states that  $\bar{k}_1^0 \equiv v\sqrt{s}/2$ , i.e., that the most energetic photon saturates all of the energy conservation alone. The function

$$\mathcal{J}(\bar{K}, v) = \frac{1}{2} \left(1 + \frac{1}{\sqrt{1 - Av}}\right), \quad \text{where} \quad A = \frac{\bar{K}^2 P^2}{(\bar{K} P)^2} \leq 1 \quad \text{and} \quad \bar{K} = \sum_{i=1}^n \bar{k}_i, \quad (2.17)$$

is a Jacobian factor left after removing the old delta function and the variable

$$\lambda_0(\bar{K}, v) = v \frac{P^2}{2\bar{K} \cdot P} \frac{2}{1 + \sqrt{1 - Av}}, \quad 0 \leq \lambda_0(\bar{K}, v) \leq 1, \quad (2.18)$$

is a solution for the rescaling factor  $\lambda$  obtained in the process of removing this old delta function. Let us notice that if there is only one photon or if the photon system has a

vanishing effective mass,  $\bar{K}^2 \rightarrow 0$ , then the two constraints, new and old, coincide; there is no need for rescaling,  $\lambda_0 \rightarrow 1$ , and the Jacobian disappears,  $\mathcal{J} \rightarrow 1$ . In fact due to the strong ordering of photon energies this is almost always the case. The other extreme situation  $A \rightarrow 1$  occurs in the case of an emission of the two antiparallel and maximally energetic photons. Finally, let us introduce the explicit polar parametrization of the photon four momenta

$$k_i = \lambda_0 \bar{k}_i = \lambda_0 \frac{\sqrt{s}}{2} x_i (1, \sin \theta_i \cos \phi_i, \sin \theta_i \sin \phi_i, \cos \theta_i), \quad (2.19)$$

which leads to

$$\frac{d^3 k_i}{k_i^0} \tilde{S}(k_i) = \frac{d^3 \bar{k}_i}{\bar{k}_i^0} \tilde{S}(\bar{k}_i) = \frac{dx_i}{x_i} d \cos \theta_i d \phi_i f(\theta_i), \quad (2.20)$$

where

$$f(\theta) = \frac{\alpha}{\pi^2} \left( \frac{1}{(1 - \beta \cos \theta)(1 + \beta \cos \theta)} - \frac{m_e^2}{s} \frac{1}{(1 - \beta \cos \theta)^2} - \frac{m_e^2}{s} \frac{1}{(1 + \beta \cos \theta)^2} \right) \quad (2.21)$$

and  $\beta = \sqrt{1 - 4m_e^2/s}$ . The final result of all the above transformations is a new form of the integral (2.13)

$$\begin{aligned} \sigma' = F_{\text{VFS}}(\epsilon) \int_{\epsilon}^{v_{\max}} dv \sigma_{\text{Born}}(s(1-v)) \int \frac{d\Omega_q}{4\pi} \left[ \delta(v) + \sum_{n=1}^{\infty} \prod_{i=1}^n \int_{\epsilon}^v \frac{dx_i}{x_i} \int_{-1}^1 d \cos \theta_i \int_0^{2\pi} d \phi_i f(\theta_i) \right. \\ \left. \delta(v - x_1) \theta(x_1 - x_2) \theta(x_2 - x_3) \dots \theta(x_{n-1} - x_n) \theta(\lambda_0(\bar{K}, v)x_n - \epsilon) \mathcal{J}(\bar{K}, v) \right]. \end{aligned} \quad (2.22)$$

It should be stressed that the above equation is completely equivalent to eq. (2.13) and in the transition from one to another we did not make any approximation nor simplification.

The distribution (2.22) could have almost been generated with the standard uniform random numbers if there was no complicated function  $\theta(\lambda_0(\bar{K}, v)x_n - \epsilon) \mathcal{J}(\bar{K}, v)$  in it. We replace it, therefore, with a simple substitute

$$\begin{aligned} \theta(\lambda_0(\bar{K}, v)x_n - \epsilon) &\longrightarrow \theta(x_n - \epsilon), \\ \mathcal{J}(\bar{K}, v) &\longrightarrow \mathcal{J}_0(v) = \frac{1}{2} \left( 1 + \frac{1}{\sqrt{1-v}} \right) \end{aligned} \quad (2.23)$$

having in mind that, as usual, it will be corrected for by the rejection. In addition, in order to ensure the stability of the rejection weights at a certain late stage of the Monte Carlo<sup>(7)</sup>

(reintroduction of  $\tilde{\beta}_1$ ) we also drop mass terms in the photon angular distribution

$$f(\theta) \longrightarrow \bar{f}(\theta) = (\alpha/\pi^2)((1 - \beta \cos \theta)(1 + \beta \cos \theta))^{-1}. \quad (2.24)$$

With the additional change of variables,  $y_i = \ln x_i$  we finally arrive at *the master integral for the Monte Carlo event generation* which defines the multidimensional distribution to be generated with the help of standard uniform random numbers

$$\begin{aligned} \sigma_{\text{crude}} = F_{\text{YFS}}(\epsilon) \int_0^{v_{\text{max}}} dv \sigma_{\text{Born}}(s(1-v)) \mathcal{J}_0(v) & \left( \delta(v) + \frac{1}{v} \sum_{n=1}^{\infty} \prod_{i=1}^n \int_{\ln \epsilon}^{\ln v} dy_i \int_{-1}^1 d \cos \theta_i \bar{f}(\theta_i) \int_0^{2\pi} d\phi_i \right. \\ & \left. \delta(\ln v - y_1) \theta(y_1 - y_2) \theta(y_2 - y_3) \dots \theta(y_{n-1} - y_n) \theta(y_n - \ln \epsilon) \right) \int \frac{d\Omega_q}{4\pi}. \end{aligned} \quad (2.25)$$

Let us explain in the following how it is actually done. Assuming for the moment that the value of the  $v$  and of the photon multiplicity  $n$  are already defined (see below for details) the properly ordered  $y_i$  variables are uniformly chosen in the  $(\ln \epsilon, \ln v)$  range, the angle  $\theta_i$  according to the  $\bar{f}(\theta_i)$  distribution in the interval  $(0, \pi)$  using for example the method of ref. [6] and the  $\phi_i$  uniformly in the  $(0, 2\pi)$  range. Photon four momenta  $\bar{k}_i$  are calculated using (2.19) and rescaled with  $\lambda_0$  from (2.18). Given  $Q = q_1 + q_2 = P - \sum k_i$  the momenta  $q_1$  and  $q_2$  are generated isotropically in the  $Q$  rest frame and transformed to the laboratory system. In this way we obtain a set of momenta  $q_1, q_2, k_1, \dots, k_n$  obeying the total four momentum conservation rule and the condition  $v = 1 - s'/s$ . The question still to be answered is: how do we generate  $v$  and  $n$ ? Let us integrate in (2.25) over all  $y_i$  and the photon angles  $\theta_i$  and  $\phi_i$ :

$$\begin{aligned} \sigma_{\text{crude}} = F_{\text{YFS}}(\epsilon) \int_0^{v_{\text{max}}} dv \sigma_{\text{Born}}(s(1-v)) \mathcal{J}_0(v) & \left( \delta(v) \right. \\ & \left. + \theta(v - \epsilon) \frac{1}{v} \sum_{n=1}^{\infty} \frac{1}{(n-1)!} \left( 2 \frac{\alpha}{\pi} \ln \frac{s}{m_e^2} \ln \frac{v}{\epsilon} \right)^{n-1} \right). \end{aligned} \quad (2.26)$$

As we see, for  $v > \epsilon$  the photon multiplicity minus one is distributed according to the Poisson distribution with the average  $2 \frac{\alpha}{\pi} \ln(s/m_e^2) \ln(v/\epsilon)$ . In order to obtain the distribution

---

(7) We would like to thank dr. Z. Was for pointing out to us this problem. See also Appendix B for more comments.

of  $v$  we have to sum over the photon multiplicity  $n$  and the result can be cast into a sum of the two  $v$ -integrals

$$\sigma_{\text{crude}} = \exp(\delta_{\text{YFS}}) \left( \int_0^\epsilon dv \gamma v^{\gamma-1} \sigma_{\text{Born}}(s) + \int_\epsilon^{v_{\text{max}}} dv \sigma_{\text{Born}}(s(1-v)) \mathcal{J}_0(v) \gamma' v^{\gamma'-1} \epsilon^{\gamma-\gamma'} \right), \quad (2.27)$$

which represent the cases  $n = 0$  and  $n > 0$  correspondingly and we define

$$\gamma = 2 \frac{\alpha}{\pi} \left[ \ln \frac{s}{m_e^2} - 1 \right], \quad \gamma' = 2 \frac{\alpha}{\pi} \ln \frac{s}{m_e^2}. \quad (2.28)$$

Note that the factor  $\epsilon^\gamma = \int_0^\epsilon \gamma v^{\gamma-1} dv$  was transferred from the YFS form-factor to the integrand and the remaining part of the form-factor is denoted as

$$\exp(\delta_{\text{YFS}}) = \exp \left( \frac{\alpha}{\pi} \left( \frac{1}{2} \ln \frac{s}{m_e^2} - 1 + \frac{\pi^2}{3} \right) \right). \quad (2.29)$$

The variable  $v$ , the central variable in the Monte Carlo is generated according to the integrand of

$$\sigma_{\text{crude}} = e^{\delta_{\text{YFS}}} \int_0^{v_{\text{max}}} dv \gamma v^{\gamma-1} \sigma_{\text{Born}}(s(1-v)) \mathcal{J}_0(v) E_{\text{mass}}(v), \quad (2.30)$$

$$\mathcal{J}_0(v) = \frac{1}{2} (1 + (1-v)^{-1/2}), \quad E_{\text{mass}}(v) = 1 + \theta(v-\epsilon) \frac{\gamma'}{\gamma} \left( \frac{v}{\epsilon} \right)^{\gamma'-\gamma}$$

and once  $v$  is known we decide that  $n = 0$  for  $v < \epsilon$  or  $n > 0$  (Poisson distribution) for  $v > \epsilon$ . The above formula is almost identical to the analogous one in ref. [8] except of the factor  $\mathcal{J}_0(v)$  which is related to the dilatation Jacobian, see eqs. (2.17) and (2.23), and the factor  $E_{\text{mass}}(v)$  which is entirely due to neglecting the electron mass terms in the photon angular distribution, see eq. (2.23). Note that the distribution  $d\sigma_{\text{crude}}/dv$  is a complicated and strongly varying function with up to three sharp peaks at  $v = 0, 1, 1 - M_Z^2/s$ . It is generated with the help of a general purpose Monte Carlo subprogram for generating an arbitrary one dimensional distribution, see Section 4 for more details, which also provides the value of the (numerically) integrated cross section  $\sigma_{\text{crude}}$ .

The events generated according to the simplified differential cross section defined in the master equation (2.25) have now to be processed through a rejection procedure in order



to remove all approximations which were made on the way from eq. (2.2) to eq. (2.25). The rejection weight

$$w = \prod_{k=1}^4 w_k \quad (2.31)$$

includes four component weights  $w_k$  which are responsible for the corresponding simplifications and we will list them below. Let us note that *the precise integrated cross section* is given by

$$\sigma = \sigma_{\text{crude}} < w >_{\text{crude}} \quad (2.32)$$

where the average weight  $< w >_{\text{crude}}$  is taken over the crude generated events, prior to rejection. The error on  $\sigma$  is determined in the usual way by the variance of the weight  $w$  and the number of the generated events.

Let us stress that the above total cross section is in our approach a result of the exact (up to statistical error) integration of the differential distribution defined in eq. (2.2) over the entire photon phase space. We doubt that the result can be ever cast into an analytical form. One may ask, however, can we gain more insight into the total and differential cross sections resulting from the Monte Carlo calculation. To this end it is very instructive to look more carefully into the  $v$ -distribution

$$\frac{d\sigma}{dv} = \frac{d\sigma_{\text{crude}}}{dv} < w >_{\text{crude}} \quad (2.33)$$

where  $d\sigma_{\text{crude}}/dv$  is known analytically, see eq. (2.30) while  $< w >_{\text{crude}}$  is calculated numerically. Since  $v$  is the first variable in the Monte Carlo generation chain it is possible to fix it and to analyse (numerically) the  $v$ -dependence of  $< w >_{\text{crude}}$  and of each individual weight  $< w_i >_{\text{crude}}$ . We refer the reader to Appendix B for more details on this interesting exercise.

Tracing back the path of all simplification on the way from eq. (2.2) to eq. (2.25) let us first define the first weight  $w_1$  which corresponds to dropping mass terms in the photon angular distribution

$$w_1 = \prod_{i=1}^n \frac{f(\theta_i)}{\bar{f}(\theta_i)} \quad (2.34)$$

In fact, this weight cancels the factor  $E_{\text{mass}}(v)$  in the  $v$  distribution, as can be verified numerically in the Monte Carlo calculation, see Appendix B for more details. In other words, for a given  $v$  we know precisely the average of  $w_1$ , i.e.,  $< w_1 >_{\text{crude}} = 1/E_{\text{mass}}(v)$ .

The next two weights correspond to the simplification made on the dilatation Jacobian and the lower photon energy boundary, see eq. (2.23),

$$\begin{aligned} w_2 &= \frac{\mathcal{J}(\bar{K}, v)}{\mathcal{J}_0(v)} = \frac{1 + (1 - Av)^{-1/2}}{1 + (1 - v)^{-1/2}} \\ w_3 &= \theta(\lambda_0(\bar{K}, v)x_n - \epsilon) = \theta\left(\frac{2k_n^0}{\sqrt{s}} - \epsilon\right). \end{aligned} \quad (2.35)$$

The fourth weight corresponds to the transition from the original distribution (2.2) to eq. (2.11)

$$\begin{aligned} w_4 &= \frac{1}{b_0} \left( \tilde{\beta}_0(\mathcal{R}p_1, \mathcal{R}p_2, \mathcal{R}q_1, \mathcal{R}q_2) \right. \\ &\quad \left. + \sum_{l=1}^n \frac{\tilde{\beta}_1(\mathcal{R}p_1, \mathcal{R}p_2, \mathcal{R}q_1, \mathcal{R}q_2, k_l)}{\tilde{S}(k_l)} + \sum_{\substack{l,j=1 \\ l \neq j}}^n \frac{\tilde{\beta}_2(\mathcal{R}p_1, \mathcal{R}p_2, \mathcal{R}q_1, \mathcal{R}q_2, k_l, k_j)}{\tilde{S}(k_l)\tilde{S}(k_j)} \right). \end{aligned} \quad (2.36)$$

There is a distinct difference between the three weights  $w_{1,2,3}$  and the weight  $w_4$ . The weight  $w_{\text{MC}} = w_1 w_2 w_3$  does not include any information on the perturbative order of the particular QED calculation nor about any other detail on the QED calculation apart from resummation of the soft photons. In a sense, the part of our program generating events according to eq. (2.11) is a general purpose MC event generator for *any type/order* QED calculation for process (2.1). This part of our generator is well isolated from the rest of the program and we call it our low level Monte Carlo (LLMC) generator. The type/order of the QED calculation is determined fully by the model weight  $w_4$  only. In particular there exists an interesting option<sup>(8)</sup> in which the first or second order QED calculation without exponentiation can also be emulated with the help of our LLMC generator by assigning a nonzero  $w_4 \neq 0$  for  $n = 0, 1$  or  $n = 0, 1, 2$  and setting  $w_4 = 0$  for higher photon multiplicities.

---

(8) This option may be used for test comparisons with the other MC programs, when available. It was already used to test the program of ref. [12].

### 3. The matrix elements and the reduction procedure

The infrared finite functions  $\tilde{\beta}_{0,1,2}$  are calculable perturbatively order by order and in this section we shall present for them the second order expressions which are actually used in the program. In order to reach the precision level defined in the Introduction it is necessary to keep the exact formula for the first order contributions but it is enough to employ the leading-logarithmic approximations for the second order contributions to  $\tilde{\beta}$ 's. The formal definitions of  $\tilde{\beta}$ 's up to second order were given in ref. [10]. In the process of the calculation we often exploited the differential cross sections from refs. [2], [3] and [16].

The second order formula for  $\tilde{\beta}_0$  includes up to two virtual photons. It is extracted, see ref. [10], from the second order expression for  $d\sigma^{(2)}/d\Omega_q$  and it reads

$$\tilde{\beta}_0^{(2)}(p_1, p_2, q_1, q_2) = \frac{d\sigma_{\text{Born}}}{d\Omega_q}(s, \theta_q) \left( 1 + \left( \frac{\alpha}{\pi} \right) (L - 1) + \frac{1}{2} \left( \frac{\alpha}{\pi} \right)^2 L^2 \right), \quad L = \ln \frac{s}{m_e^2}, \quad (3.1)$$

where  $d\sigma_{\text{Born}}/d\Omega$  is the lowest order differential cross section. It should be noted that the above formula is considerably simpler than the original second order differential cross section, notably it does not include any large double logarithmic corrections which have been summed up into the Yennie-Frautschi-Suura (Sudakov) formfactor, see eq. (2.5). The vacuum polarization contribution was not included since it is understood to be included in the  $Z^0$  and  $\gamma$  propagators. The contribution from the light fermion pair production, numerically small [3], was neglected. The first order formula for  $\tilde{\beta}_0$  was already given in ref. [9]. Reinstallation of the remaining nonleading second order corrections in the above expression would be rather straightforward since all necessary ingredients are given in ref. [2]. The zero-th and the first order versions  $\tilde{\beta}_0^{(0)}$  and  $\tilde{\beta}_0^{(1)}$  are obtained by truncating the higher order terms in the above expression.

The second order  $\tilde{\beta}_1$  includes one real photon and the contributions from up to one virtual photon. It will be defined with the help of the corresponding differential cross section

$$D_1^{(2)}(p_1, p_2, q_1, q_2, k) = \frac{\alpha}{4\pi^2} \frac{2p_1 p_2}{(kp_1)(kp_2)} \left[ 1 + \left( \frac{\alpha}{\pi} \right) (L - 1) \left( 1 + \frac{1}{2} \ln(1 - \hat{\alpha} - \hat{\beta}) \right) \right] \quad (3.2)$$

$$\frac{1}{2} \left( (1 - \hat{\alpha})^2 \frac{d\sigma_{\text{Born}}}{d\Omega_q}(s', \theta_{q,1}) + (1 - \hat{\beta})^2 \frac{d\sigma_{\text{Born}}}{d\Omega_q}(s', \theta_{q,2}) \right) W_m(\hat{\alpha}, \hat{\beta}),$$

where

$$W_m(\hat{\alpha}, \hat{\beta}) = 1 - \frac{m_e^2}{s} \frac{2(1 - \hat{\alpha})(1 - \hat{\beta})}{(1 - \hat{\alpha})^2 + (1 - \hat{\beta})^2} \left( \frac{\hat{\alpha}}{\hat{\beta}} + \frac{\hat{\beta}}{\hat{\alpha}} \right), \quad \hat{\alpha} = \frac{kp_2}{p_1 p_2}, \quad \hat{\beta} = \frac{kp_1}{p_1 p_2} \quad (3.3)$$

and the normalization constant is such that  $D_1^{(2)} \rightarrow \tilde{S}(k)\tilde{\beta}_0^{(1)}$  for  $k \rightarrow 0$ . Neglecting the  $(\alpha/\pi)^2$  contribution leads us to the well known single bremsstrahlung matrix element with the following definition of the angles  $\theta_{q,i}$  [17]: The  $\theta_{q,1}$  is taken in the rest frame of the  $q_1 + q_2$  as a polar angle of the  $\vec{q}_1$  with respect to  $z$ -axis pointing along  $\vec{p}_1$  in this frame while  $-\vec{p}_2$  is used as a  $z$ -axis for  $\theta_{q,2}$ . The  $\hat{\alpha}$  and  $\hat{\beta}$  are Sudakov (light-cone) variables which in the collinear situations have the following simple meaning: If  $e^-(p_1)$  fragments almost collinearly into a photon with a momentum fraction  $zp_1$  and a quasi-real electron of momentum  $(1-z)p_1$  then  $\hat{\alpha} = z$  and  $\hat{\beta} \simeq 0$ . In this case the above distribution reduces to the Altarelli-Parisi [18] splitting function times the lowest order differential cross section

$$D_1^{(1)}(p_1, p_2, q_1, q_2, k) \sim \left(\frac{\alpha}{\pi}\right) \frac{1 + (1-x)^2}{2x} \frac{d\sigma_{\text{Born}}(s', \theta_q)}{d\Omega_q}, \quad (3.4)$$

which is the result expected in the leading-log approximation. Analogously, in the case of  $e^+$  fragmentation  $\hat{\alpha} \simeq 0$  and  $\hat{\beta} = z$ . Note also that the distinction between  $\theta_{q,1}$  and  $\theta_{q,2}$  disappears in the collinear regions. The second order contribution in the above formula is written in the collinear approximation. It can either be taken directly from ref. [2] or obtained by convoluting the Altarelli-Parisi function with itself [3]. Finally, the leading-logarithmic expression<sup>(9)</sup> for  $\tilde{\beta}_1$  is defined as follows [7,10]

$$\tilde{\beta}_1(p_1, p_2, q_1, q_2, k) = D_1^{(2)}(p_1, p_2, q_1, q_2, k) - \tilde{S}(p_1, p_2, k)\tilde{\beta}_0^{(1)}(\mathcal{R}p_1, \mathcal{R}p_2, \mathcal{R}q_1, \mathcal{R}q_2). \quad (3.5)$$

The above expression is manifestly finite in the  $k \rightarrow 0$  infrared limit. As we see, the reduction procedure for  $\tilde{\beta}_0$  (see previous Section for its definition) necessarily enters into the definition of  $\tilde{\beta}_1$ . It must be so since  $\tilde{\beta}_0$  is originally defined within the two body phase space only. Let us remark on the important property of the  $\tilde{\beta}_1$  contribution in the sum of the eq. (2.2)

$$\tilde{\beta}_0(\mathcal{R}p_1, \mathcal{R}p_2, \mathcal{R}q_1, \mathcal{R}q_2) + \sum_{l=1}^n \frac{\tilde{\beta}_1(\mathcal{R}p_1, \mathcal{R}p_2, \mathcal{R}q_1, \mathcal{R}q_2, k_l)}{\tilde{S}(p_1, p_2, k_l)}. \quad (3.6)$$

As a direct consequence of the definition of  $\tilde{\beta}_1$  the second term (sum over  $\tilde{\beta}_1$ 's) does not contribute at all if there is no hard photon (its relative contribution is in fact less than  $10^{-3}$  for  $v < 0.001$ ). On the other hand, if there is one and only one,  $l$ -th, hard photon

---

(9) The precise second order formula for  $D_1^{(2)}$  cannot be found in the literature (in ref. [2] the integration over photon angle and  $d\Omega_q$  was performed), but it is definitely calculable.

then the corresponding  $\tilde{\beta}_1(k_l)$  is dominant and the differential distribution  $D_1(k_l)$  for this photon effectively replaces the whole above expression. The first  $\tilde{\beta}_0$  in (3.6) and the  $\tilde{\beta}_0$  inside  $\tilde{\beta}_1(k_l)$  cancel each other. If there are two or more hard photons then, in this part of the phase space, the above expression is not adequate any more, and only the inclusion of  $\tilde{\beta}_2, \tilde{\beta}_3 \dots$  may improve the situation.

For practical calculations the definition of  $\tilde{\beta}_1$  must be immediately supplemented with the corresponding definition of the reduction procedure  $\mathcal{R}$  specific for  $\tilde{\beta}_1$ . It appears that, for  $\tilde{\beta}_{1,2}$ , in addition to conditions (2.6) and (2.10) there is another constraint on the way it is defined. As discussed above, in the sum (3.6) the contribution

$$\frac{\tilde{S}(\mathcal{R}p_1, \mathcal{R}p_2, \mathcal{R}k_l)}{\tilde{S}(p_1, p_2, k_l)} \tilde{\beta}_0(\mathcal{R}^2 p_1, \mathcal{R}^2 p_2, \mathcal{R}^2 q_1, \mathcal{R}^2 q_2) \simeq \frac{(k_l)_T^2}{(\mathcal{R}k_l)_T^2} \tilde{\beta}_0(\mathcal{R}^2 p_1, \mathcal{R}^2 p_2, \mathcal{R}^2 q_1, \mathcal{R}^2 q_2),$$

is present. In the case when  $l$ -th photon is hard this contribution should be matched (canceled) by the  $\tilde{\beta}_0(\mathcal{R}p_1, \mathcal{R}p_2, \mathcal{R}q_1, \mathcal{R}q_2)$ . This means that to a very good approximation the reduction procedure for  $\tilde{\beta}_0$  should be idempotent, i.e.,  $\mathcal{R}^2 = \mathcal{R}$  and, furthermore, for  $\tilde{\beta}_1$  it should preserve the transverse component  $k_T^2 \simeq (kp_1)(kp_2)/(p_1 p_2)$  of the photon momentum with respect to  $p_1$  and  $p_2$ . To satisfy all these requirements we proceed as follows. Let us suppose that we want to eliminate all photons except the  $l$ -th one. With the  $z$ -boost along the beam move to a frame where  $(q_1 + q_2 + k_l)^3 = 0$  and we pretend that there is no other photon except  $k_l$ , as in the second equation of (2.6). We define  $\mathcal{R}(\vec{q}_1 + \vec{q}_2) = \mathcal{R}\vec{Q} \equiv -\vec{k}_l$  in this frame. Then we assign  $\mathcal{R}Q^0 \equiv ((\mathcal{R}\vec{Q})^2 + s')^{-1/2}$  and  $\mathcal{R}P = \mathcal{R}Q - k_l$ . Obviously, we have obtained  $\mathcal{R}P = \mathcal{R}Q + k_l$ , i.e. the condition (2.6) is fulfilled. Since  $\mathcal{R}\vec{P} = \mathcal{R}\vec{p}_1 + \mathcal{R}\vec{p}_2 = \vec{0}$  we easily define new (effective) beam momenta  $\mathcal{R}p_1$  and  $\mathcal{R}p_2$  along the  $z$ -axis and the only thing to be still done is to define  $\mathcal{R}q_i$  satisfying  $\mathcal{R}Q = \mathcal{R}q_1 + \mathcal{R}q_2$ , where  $\mathcal{R}Q$  is known already. It practically means that we have to define  $\mathcal{R}q_i$  in the rest frame of  $\mathcal{R}Q$  and to transform them back to the laboratory reference frame. In order to ensure the idempotence of the reduction procedure  $\mathcal{R}^2 = \mathcal{R}$  we choose the vectors  $\mathcal{R}q_i$  in the same way as in the case of the reduction operation for  $\tilde{\beta}_0$  described in the previous Section, i.e., we make a boost along the longitudinal and the transverse part of  $Q = q_1 + q_2$  and take for  $\mathcal{R}q_i$  the resulting  $q_i$  in  $Q$  rest frame. The exact idempotence of  $\mathcal{R}$  for  $\tilde{\beta}_0$  saves us also considerably in computing time since  $\tilde{\beta}_0$  is calculated only once and the result is used many times. Let us finally note, that the above reduction procedure differs from what was used in the earlier version of the program described (partly) in the ref. [9] where the condition (2.10) was not imposed and the  $p_i$  momenta were not touched;  $\mathcal{R}p_i = p_i$ . In this case the effective shift  $s \rightarrow s'$  in  $Z^0$  propagator in  $d\sigma_{\text{Born}}$  in (3.6) was due

to the emission of only one (the hardest) photon. Such a procedure is perfectly sufficient for the Born cross section mildly dependent on  $s$  but in the case of the very strong dependence it hinders the precision of the resulting corrected cross section. In the referred case we could only reach about 1 – 2% precision level near the  $Z^0$  resonance.

The second order double bremsstrahlung matrix element, being a raw material for the construction of  $\tilde{\beta}_2$ , does not contain any virtual correction and in the leading-log/collinear approximation may be written in a following compact form

$$D_2^{(2)}(p_1, p_2, q_1, q_2, k_1, k_2) = \frac{\alpha}{4\pi^2} \frac{2p_1 p_2}{(k_1 p_1)(k_1 p_2)} \frac{\alpha}{4\pi^2} \frac{2p_1 p_2}{(k_2 p_1)(k_2 p_2)} \cdot \frac{1}{8} \left( f_1(\hat{\alpha}_i, \hat{\beta}_i) \frac{2d\sigma_{\text{Born}}}{d\Omega_q}(s', \theta_{q,1}) + f_2(\hat{\alpha}_i, \hat{\beta}_i) \frac{2d\sigma_{\text{Born}}}{d\Omega_q}(s', \theta_{q,2}) \right) W_m(\hat{\alpha}_1, \hat{\beta}_1) W_m(\hat{\alpha}_2, \hat{\beta}_2) \quad (3.7)$$

where

$$\begin{aligned} \text{for } \hat{\alpha}_1 + \hat{\beta}_1 > \hat{\alpha}_2 + \hat{\beta}_2 \quad & \begin{cases} f_1(\hat{\alpha}_i, \hat{\beta}_i) = Y(\hat{\alpha}_1; \hat{\alpha}'_2, \hat{\beta}'_2) + Y(\hat{\alpha}'_1; \hat{\alpha}_2, \hat{\beta}_2), \\ f_2(\hat{\alpha}_i, \hat{\beta}_i) = Y(\hat{\beta}_1; \hat{\alpha}'_2, \hat{\beta}'_2) + Y(\hat{\beta}'_1; \hat{\alpha}_2, \hat{\beta}_2), \end{cases} \\ \text{for } \hat{\alpha}_1 + \hat{\beta}_1 \leq \hat{\alpha}_2 + \hat{\beta}_2 \quad & \begin{cases} f_1(\hat{\alpha}_i, \hat{\beta}_i) = Y(\hat{\alpha}_2; \hat{\alpha}'_1, \hat{\beta}'_1) + Y(\hat{\alpha}'_2; \hat{\alpha}_1, \hat{\beta}_1), \\ f_2(\hat{\alpha}_i, \hat{\beta}_i) = Y(\hat{\beta}_2; \hat{\alpha}'_1, \hat{\beta}'_1) + Y(\hat{\beta}'_2; \hat{\alpha}_1, \hat{\beta}_1), \end{cases} \end{aligned}$$

$$Y(x, u, v) \equiv (1 - x)^2 [(1 - u)^2 + (1 - v)^2],$$

$$\hat{\alpha}_i = \frac{k_i p_2}{p_1 p_2}, \quad \hat{\beta}_i = \frac{k_i p_1}{p_1 p_2}, \quad \hat{\alpha}'_1 = \frac{\hat{\alpha}_1}{1 - \hat{\alpha}_2}, \quad \hat{\alpha}'_2 = \frac{\hat{\alpha}_2}{1 - \hat{\alpha}_1}, \quad \hat{\beta}'_1 = \frac{\hat{\beta}_1}{1 - \hat{\beta}_2}, \quad \hat{\beta}'_2 = \frac{\hat{\beta}_2}{1 - \hat{\beta}_1}.$$

In the collinear region the two photons may be emitted both from the  $e^-$  beam, both from the  $e^+$  beam or each one from a different beam. It is easy to see that in each of these cases the above formula coincides with the appropriate convolution of the two Altarelli-Parisi fragmentation functions. For example for a double collinear fragmentation of

$$e^-(p_1) \rightarrow \gamma(z_1 p_1) + e^-((1 - z_1)p_1) \rightarrow \gamma(z_1 p_1) + [\gamma(z_2(1 - z_1)p_1) + e^-((1 - z_2)(1 - z_1)p_1)]$$

we have  $x_i = 2k_i^0/s^{1/2} = \hat{\alpha}_i$  and  $\hat{\beta}_i \simeq 0$  but  $\hat{\alpha}_1 = z_1$   $\hat{\alpha}'_1 = z_2$  and, assuming  $\hat{\alpha}_1 > \hat{\alpha}_2$ , the corresponding factor in  $f_1 + f_2$  (note that  $\theta_{q,1} \simeq \theta_{q,2}$ ) reads

$$Y(\hat{\alpha}_1; \hat{\alpha}'_2, \hat{\beta}'_2) + Y(\hat{\beta}_1; \hat{\alpha}'_2, \hat{\beta}'_2) = (1 + (1 - z_1)^2)(1 + (1 - z_2)^2)$$

as expected from convoluting two Altarelli-Parisi functions. The other two terms in  $f_1 + f_2$  result from Bose symmetrization. In a similar way one may check the proper behavior of

$D_2$  in the case of the double fragmentation of the  $e^+$  and in the case of the independent single fragmentation of  $e^+$  and  $e^-$ . All that is very much in the spirit of refs. [3] and [4] but with two improvements relative to them. First of all the proper infrared limit is reproduced  $D_2^{(2)} \rightarrow \tilde{S}(k_1)\tilde{S}(k_2)\tilde{\beta}_0^{(0)}$  for  $k_1, k_2 \rightarrow 0$ . And secondly, in the case when one photon is hard collinear and the other hard non-collinear then our distribution still applies there. It factorizes into an Altarelli-Parisi fragmentation for the collinear photon times the exact single bremsstrahlung differential cross section at the reduced c.m.s. frame for the noncollinear one. To this end we had to introduce the two angles  $\theta_{q,i}$  in  $D_1^{(2)}$ . Our distribution does not apply to the situation with the two hard noncollinear (high  $p_T$ ) photons. Although the above leading-log approximation is sufficient for all of the practical applications one could also use the exact double bremsstrahlung matrix element calculated using spin amplitudes and spinorial technique of ref. [19]. This should be done at a certain point as a test for the above simple expression. The final expression for  $\tilde{\beta}_2$  [7,10] reads

$$\begin{aligned} \tilde{\beta}_2(p_i, q_j, k_1, k_2) = & D_2^{(2)}(p_i, q_j, k_1, k_2) \\ & - \tilde{S}(p_i, k_1)\tilde{\beta}_1^{(1)}(\mathcal{R}p_i, \mathcal{R}q_j, k_2) - \tilde{S}(p_i, k_2)\tilde{\beta}_1^{(1)}(\mathcal{R}p_i, \mathcal{R}q_j, k_1) \\ & - \tilde{S}(p_i, k_1)\tilde{S}(p_i, k_2)\tilde{\beta}_0^{(0)}(\mathcal{R}p_i, \mathcal{R}q_j) \end{aligned} \quad (3.8)$$

where the reduction enters again, in both  $\tilde{\beta}_0$  and  $\tilde{\beta}_1$ . In the sum

$$\tilde{\beta}_0(\mathcal{R}p_i, \mathcal{R}q_j) + \sum_{l=1}^n \frac{\tilde{\beta}_1(\mathcal{R}p_i, \mathcal{R}q_j, k_l)}{\tilde{S}(p_i, k_l)} + \sum_{\substack{l,m=1 \\ l \neq m}}^n \frac{\tilde{\beta}_2(\mathcal{R}p_i, \mathcal{R}q_j, k_l, k_m)}{\tilde{S}(p_i, k_l)\tilde{S}(p_i, k_m)} \quad (3.9)$$

the contribution from the third term (sum over  $\tilde{\beta}_2$ 's) is a small contribution except of the situation when there are two hard photons simultaneously. Then, one of  $\tilde{\beta}_2$  contributions overtakes the whole expression and introduces the proper  $D_2$  distribution in this region of the phase space. Again, this distribution will not be very good if there are three hard photons (or two hard non-collinear photons). The contributions to the total cross-section from these regions of the phase space are known to be extremely small. If, however, one day it will appear to be necessary to introduce the precise matrix element for three photons then the corresponding modification of our program will be quite straightforward. Only this part of the program which provides weight  $w_4$  will have to be corrected. The rest of the program (LLMC generator) will remain unchanged.

The reduction procedure for  $\tilde{\beta}_2$  is defined very similarly as in the case of  $\tilde{\beta}_1$ . We go with help of  $z$ -boost to a frame where  $(q_1 + q_2 + k_i + k_l)^3 = 0$  and then construct  $\mathcal{R}p_i$  and  $\mathcal{R}q_i$  in the same way as for  $\tilde{\beta}_1$ .

#### 4. The structure of the program – subprograms, variables

In this Section we provide some general information on the program and on its most important subprograms and we list the names of some important and most frequently used variables.

The program is divided functionally and topographically into four parts which are given the nicknames: (i) EXPAND – The main subprogram administering input/output and the main rejection loop due to the main weight  $w$ ; (ii) YFSGEN – the low level Monte Carlo generator generating the simplified distribution defined in eq. (2.13), i.e., the phase space with the importance sampling for the bremsstrahlung peaks and the  $Z^0$  resonance; (iii) MODEL – the part of the program calculating the model matrix element, i.e., the weight  $w_4$ ; and (iv) EXPLIB – the library of utilities. In the following we shall describe briefly all these parts and give short descriptions of the most important subprograms. Each of these subprograms includes a short comment explaining its role and the meaning of its parameters.

The part EXPAND consists of subroutines EXPAND and FILEXP. The first one is the main subroutine in the program. Its first parameter MODE, as also in many other subprograms, tells the subprogram if it is called in the initialization mode (MODE=-1) production/generation mode (MODE=0) or the final post-generation mode (MODE=1). The user must call on this subprogram, with MODE=0, in order to generate each Monte Carlo event but before the first event is generated he must call on it with MODE=-1 in order to provide the input data through its parameters. The input parameters are transferred to FILEXP which distributes them all over the various common blocks. FILEXP sets also the values of some other parameters in the program like input/output unit numbers, electron mass, the polarizations of  $e^\pm$  beams etc. After the last event is generated, the call on EXPAND with MODE=1 provides the value of the total cross section and a large amount of other useful information. The EXPAND makes all sorts of book-keeping on the weights, it checks also if the weights have expected properties and compares the total Monte-Carlo cross section with the estimates obtained using analytical and Gauss integrations. See the next Section for more details on the input/output organization.

The part nicknamed YFSGEN is the low-level Monte-Carlo generator which generates the multiphoton events according to the simplified distribution (2.11). The main administration subprogram is here KARLUD which also features the three-fold operation mode. It generates the variable  $v$  with help of the routine VESKO from the part EXPLIB. VESKO is the general purpose program for generating any distribution and the  $v$ -distribution is



defined by the function FUNSKO. In fact the  $v$ -distribution of eq. (2.30) is encoded in the function VVDIS. In order to flatten the peaks at  $v = 0$  and  $v = 1$  we make the appropriate change of the variables with the help of the function CHBIN2. No such provision is made for the  $Z^0$  peak. KARLUD is the administrative subprogram, it mainly does the weight book-keeping and the most of the Monte Carlo algorithm is in fact contained in the subroutine KARLUD. It essentially generates the integrand of (2.13) for fixed  $v$ . Since  $v$  is already known it, therefore, sets the photon multiplicity  $n = 0$  when  $v < \epsilon$  or, otherwise, it generates  $n$  according to a Poisson distribution with the help of the routine POISSG. In the latter case ( $v > \epsilon$ ) the photon momenta  $\bar{k}_i$  are constructed by calling on the routine BREMUL and the solution for the rescaling factor  $\lambda_0(\bar{K}, v)$  and the Jacobian factor  $\mathcal{J}(\bar{K}, v)$  is provided by the routine RESOLII. Once the photon momenta  $k_i = \lambda_0 \bar{k}_i$  are known then YFSGEN calls on the routine KINEKR which defines the fermion momenta  $q_i$ . The subroutine YFSGEN defines also the three weights  $w_1, w_2$  and  $w_3$  which are transferred to KARLUD, and later to EXPAND. The subprogram ANGBRE is called in BREMUL and it generates the photon angle  $\theta_i$  according to distribution  $\bar{f}(\theta_i)$ . It also provides the ratio  $f(\theta_i)/\bar{f}(\theta_i)$  which is a component of the weight  $w_1$ . The whole event, i.e.,  $n, k_i$  and  $q_i$ , is stored in the common block MOMSET. In the case of any improvement on the matrix element for the initial state bremsstrahlung, for example, the inclusion of the proper matrix element for more hard photons, or the inclusion of the higher order virtual and/or electroweak corrections, this part (YFSGEN) of the program will remain unchanged.

The model dependent weight  $w_4$  is provided by the part called MODEL. It is calculated according to formula (2.36) in the routine MODEL2. In fact this subprogram provides four versions of the weight  $w_4$  and the filter-routine MODEL selects one of them, the second order expression (2.36), as the principal model weight in our program. The MODEL defines also the maximum weight for the rejection in the main rejection loop in EXPAND, specific to a chosen type of the model weight. As it is also explained in a comment in the MODEL2, the following versions of the weight  $w_4$  are also provided: the weights with formula (2.36) truncated to  $\tilde{\beta}_1$  and to  $\tilde{\beta}_0$  only, but in both cases the second order expressions are taken, and the weight in which the sum in (2.36) is truncated to  $\tilde{\beta}_1$  terms and the first order calculation is applied. The EXPAND calculates the averages of these weights and prints the values of the total cross sections corresponding to all above weights, see Section 6 and Appendix B. This is very useful for the control of the precision of the total cross section obtained with the full weight as defined in eq. (2.36). The various components in the sum (2.36) are calculated by the following subprograms:  $b_0$  is provided by GCRUDE,  $\tilde{\beta}_0$  by

GBETA0,  $\tilde{\beta}_1(k_l)/\tilde{S}(k_l)$  by GBETA1 and  $\tilde{\beta}_2(k_l, k_j)/\tilde{S}(k_l)\tilde{S}(k_j)$  by GBETA2. The GBETA0 routine calls on BVIRT0 which calculates the virtual part of  $\tilde{\beta}_0$  (see the bracket factor in eq. (3.1)) and on REDUM0 which performs the reduction procedure. The GBETA1 routine uses BVIRT1 to calculate the virtual part of  $\tilde{\beta}_1$  and REDUM1 to perform the reduction procedure. Finally, the GBETA2 calls on REDUM2 which performs the corresponding reduction procedure. Among various small routines providing elements of the expressions for  $\tilde{\beta}_{1,2}$  there is GTHETA which calculates the two angles  $\theta_{q,i}$ . The function BORNV provides the lowest order differential cross section  $\sigma_p^{-1} d\sigma_{\text{Born}}/d\Omega(\theta, s)$ , where  $\sigma_p = 4\pi\alpha^2/3s$  enters in many places, in all  $\tilde{\beta}$ 's. The function BORNY calculates the integrated Born cross section (also in  $\sigma_p$  units) with the help of BORNV employing a relation

$$\sigma_{\text{Born}} = \frac{2}{3} \left( \frac{d\sigma_{\text{Born}}}{d\cos\theta}(1, s) + \frac{d\sigma_{\text{Born}}}{d\cos\theta}(-1, s) \right),$$

which is valid for any distribution of the type  $c_1(1 + \cos\theta)^2 + c_2(1 - \cos\theta)^2$ . The fermion charge and the weak isospin, used in BORNV to calculate the coupling constants, is calculated in GIVIZ0.

The most important routines in the utility library EXPLIB are the general purpose routine VESKO which is used to generate the variable  $v$  and the routine WMONIT which is used in several subprograms to monitor various weights. It calculates the average, the variance and counts abnormal weights: negative, above a certain limit, etc. The EXPLIB includes also the random number generator RANMAR from ref. [20] and the routine GAUSS for the numerical Gauss integration.

The vocabulary of the most frequently used variables is listed in the Table 1. We indicate whether the listed variable is a member of a common block. Let us finally note that, as usual in this type of the program, the whole program is written in the double precision arithmetic – mostly due to the smallness of the electron mass. There is only a very limited use of the double complex arithmetic, i.e., only for the  $Z^0$  propagator.

## 5. How to use the program – its applicability area

In the first part of this Section we shall explain how to use the program, what are the input parameters and where to look for the output. Then, we shall explain what type of the physical measurables, cross sections, distributions, asymmetries may be calculated with the help of our program. We list the effects which are omitted in the program, indicating a rough precision levels at which they start to play a role. We also instruct the user in how to include the pure electroweak corrections.

A typical sequence of instruction needed to generate a thousand of the Monte Carlo events may look as follows

```

IMPLICIT DOUBLE PRECISION (A-H,O-Z)
COMMON / MOMSET / QF1(4),QF2(4),SPHUM(4),SPHOT(100,4),NPHOT
DIMENSION XPAR(20),NPAR(20)
{ assign XPAR and NPAR }
CALL EXPAND(-1,CMSENE,XPAR,NPAR)
DO 100 IEV=1,1000
CALL EXPAND( 0,CMSENE,XPAR,NPAR)
{ histograming }
100 CONTINUE
CALL EXPAND( 1,CMSENE,XPAR,NPAR)
XSEC=XPAR(10)

```

The input parameters are read only for  $\text{MODE}=-1$ . The parameter CMSENE is the total center of the mass energy in GeV units and the other input parameters are encoded in the two arrays NPAR and XPAR. The user must necessarily define seven entries in these arrays, see the list below for a detailed description:

Entry	Name	Description
NPAR(1)	KEYRAD	=2,3 for QED first, second order
XPAR(1)	AMAZ	$M_Z$ , mass of the $Z^0$
XPAR(2)	SINW2	$\sin^2 \theta_W$ , $\theta_W$ is the electroweak mixing angle
XPAR(3)	GAMMZ	$\Gamma_Z$ , width of $Z^0$
XPAR(5)	AMFIN	$m_f$ , mass of the final fermion
XPAR(6)	VVMIN	$\epsilon$ , infrared cut-off, dimensionless
XPAR(7)	VVMAX	$v_{max}$ , maximum of $v$ variable

All these parameters are read only for  $\text{MODE}=-1$  and they are ignored in the production mode,  $\text{MODE}=0$ . The output fermion and photon momenta are provided to the user in the

common block /MOMSET/, see also Table 1. They are in *GeV* units. The momentum  $q_1^\mu$  of the fermion  $f$  is stored in the matrix QF1(K),  $K=1,2,3,4$ , with the usual convention that QF1(4) is the energy. Similarly for the fermion  $\bar{f}$  the  $q_2$  is given by QF2. The momentum of the  $i$ -th photon  $k_i$  is placed in the SPHOT( $i,K$ ),  $K=1,2,3,4$ . The third axis is pointed in the direction of  $e^-$  momentum  $\vec{p}_1$ . The photon multiplicity is provided as NPHOT. Once the histograming is done the user may want to normalize the distributions to a proper integrated cross section  $\sigma$ . It can be found in XPAR(10); the other elements of XPAR and NPAR may also be of some interest, see the following list:

Entry	Name	Description
XPAR(10)	XSMC	$\sigma$ integrated Monte Carlo cross section in units of $4\pi\alpha^2/3s$
XPAR(11)	EREL	relative error on $\sigma$ , estimated from the variance of the weight
XPAR(12)	XSMCNB	$\sigma$ in nanobarns
NPAR(10)	NEVTOT	number of the generated events

The call on EXPAND with MODE=1 automatically produces printout of about 50 control parameters with various pieces of useful information. We shall give a more detailed description of them in the next Section and in Appendix B. This printout may be avoided if one calls on EXPAND with MODE=2. In this case the parameters XPAR and NPAR are defined as for MODE=1.

Let us now comment on the applicability range of the program. As stated above (see also next Section), the program may be used to calculate the effects related to the initial state QED bremsstrahlung on the total cross section and related quantities with the precision below 0.5%. Can we really talk about such a precision from the point of view of the QED, electroweak corrections and QCD influence? The QED case looks good because the contribution from the omitted final state bremsstrahlung on the total cross section is only  $\delta\sigma/\sigma = \frac{3}{4}\alpha/\pi = 0.003$ .<sup>(10)</sup> The influence of the initial/final state interference on the unpolarized cross section is also small,  $\delta\sigma/\sigma \simeq 2 \cdot 10^{-5}$  on the  $Z^0$  peak and up to  $\simeq 7 \cdot 10^{-4}$  away from the peak [21]. The omitted second order contribution from the production of the light fermion pairs (going mostly into beam pipe) is about  $\delta\sigma/\sigma \simeq 0.003 - 0.005$  see refs. [22,23,3]. Our program, as it stands, has nothing to say about the other kinds of the corrections. The parameters like  $Z^0$  width, couplings parametrized with  $\sin^2\theta_W$  are the external entities. The pure electroweak corrections contribute to the total cross

---

(10) The final state bremsstrahlung may become quite important in the presence of strong cut-offs.

section in principle at the level of  $\delta\sigma/\sigma \simeq \alpha/\pi \simeq 0.003$ . It is known, however, that the QCD corrections to the total cross sections, entering mainly through the  $Z^0$  width, are in a percent range. One may hope that at some point the total cross section on the  $Z^0$  resonance can be predicted from the standard model at the 1% level [22]. The precision capabilities of the presented program are definitely better than that.

The situation looks better for the initial state polarization asymmetry  $A_{LR}$ . Many uncertainties like the influence of the final state QCD and QED radiation cancels out [21],  $\delta A_{LR} \leq 0.001$  near the  $Z^0$  position, and are below the anticipated experimental precision level 0.003. The presented program is therefore well suited for this purpose. One has only to attach to this program the library of the electroweak corrections in a reasonable way. There are several possible ways to do it. One of them, advocated in ref. [24], is rather easy to implement – the electroweak corrections are included in the Born differential cross section which is (in the leading-logarithmic approximation) a basic building block for all differential cross sections. For more details see the latter part of this Section. A possible worry about this procedure may be related to the improper treatment of the helicity non-conserving components in the differential cross sections. These contributions are, however, known to be  $\delta A_{LR} \leq 10^{-4}$  (for  $v < 0.9$ ) at the  $Z^0$  position and are also below the experimental precision level [21].

Can this program, provided that electroweak corrections are added, be used to calculate the forward/backward asymmetry  $A_{FB}$ ? Outside the  $Z^0$  peak definitely not, because the effects due to the initial/final state interference induces  $\delta A_{FB} \simeq +1.5\%$  or even more and this is neglected in our program. It appears, however, that at the top of the  $Z^0$  this contribution is suppressed very much, provided one does not apply stringent cut-offs on the photon momenta. If one accepts events with photons up to 20% of the beam energy then at the  $Z^0$  position this contribution to  $A_{FB}$  is less than 0.001, see ref. [25]. The other type of the pure QED influence on  $A_{FB}$  comes from the shift of the effective center of the mass energy  $\sqrt{s}$  due to the initial state bremsstrahlung combined with the rapid dependence of  $A_{FB}$  on  $s$ . Since our program provides a very good control on the total cross section this effect can be, therefore, calculated with its help quite precisely. Summarizing, one may use this program to calculate  $A_{FB}$  close ( $M_Z \pm 1\text{GeV}$ ) to the  $Z^0$  position provided that cut-offs are very loose. A complete calculation of the QED effects will be possible with the next version of the present program [26] which will include the final state bremsstrahlung and the final/initial state interference.

The case of the third asymmetry – spin polarization with respect to the final state polarization  $A_{pol}$  measured in the  $\tau$  pair production process is the most difficult because

in this case one definitely needs the emission of the photon from the outgoing  $\tau$ 's [27,28]. The program in the present form is not useful for this measurement. Here we recommend that the reader uses a temporary solution which is provided within the unpublished but available program KORALZ, version 3.x, which includes the single photon emission from the final state (no interference) in addition to multiphoton effects of this program. The real solution will come again with the future development of the presented multiphoton program.

Let us come to the question how to introduce easily and efficiently the electroweak corrections into the present program. The simplest way [24] is to replace the subprogram BORNV which provides the differential lowest order cross section with the new one providing the corrected distribution

$$\frac{1}{\sigma_p} \frac{d\sigma_{\text{Born}}}{d\Omega}(\theta, s) \longrightarrow \frac{1}{\sigma_p} \frac{d\sigma_{\text{EW}}}{d\Omega}(\theta, s),$$

One should also provide a separate new function BORNs, independent of BORNV, for the integrated corrected cross section  $\sigma_{\text{Born}}$ , which enters into  $d\sigma_{\text{crude}}/dv$  and into  $b_0$ , see routines VVDIS and GCRUDE. For the sake of the weight stability this cross section should have the  $Z^0$  propagator parametrized in way close to that in  $d\sigma_{\text{EW}}/d\Omega$ . Since both the electroweak corrected distribution  $d\sigma_{\text{EW}}/d\Omega(\theta, s)$  will be called many times for various values of  $s$  and the  $\theta$ , therefore, a pretabulation procedure (look-up tables) of the electroweak corrections as a function of these variables is strongly recommended in order to speed up the calculations.

Summarizing, the present program is very well suited for studies on the total cross section and the initial state polarization  $A_{LR}$ . With some restrictions it can be used for the charge asymmetry  $A_{FB}$  and it is not yet up to standards required for the final state asymmetry  $A_{pol}$ .

## 6. Examples of numerical results

In this Section we shall show the examples of numerical results from our program, mainly for the total cross section – concentrating on the question of the precision of our program. We also explain where the presented results may be found in the output of the program. Included are also two distributions which can be obtained with our program and which cannot be obtained with any other Monte Carlo program which does not feature the proper resummation over the soft photons. More examples of the numerical results will be presented elsewhere.

The results for the total cross section are presented in the Tables 2 and 3. In Table 1 we show the total cross section and the various related quantities for three energies close to the  $Z^0$  position. All these quantities can be read directly from the output from the routine EXPAND, called at the end of the generation run with MODE=1. They can be easily found in the printout, see the excerpts from the test output included at the end of the paper. The printout from EXPAND is divided into three windows A, B and C and each window includes several items marked with A1, A2, A3, ..., B1, B2, ... etc. For example the principal total cross section in nanobarns is printed in window A position A2. We included these marks in the Tables. In fact these two Tables in themselves constitute a useful test of the program which may help to verify whether the program functions properly.

Generally, the precision of the perturbative calculation can be deduced from the convergence of the perturbative series. In our case we have already summed up the contributions from the soft photons up to infinite order and what remains is, in a sense, the expansion in a number of “hard/noninfrared” photons. This is represented in our master equation (2.2) by a series in  $\tilde{\beta}$ ’s and our best second order cross section  $\sigma = \sigma(\tilde{\beta}_0 \oplus \tilde{\beta}_1 \oplus \tilde{\beta}_2)$ , see Table 2, involves the sum  $\tilde{\beta}_0 + \sum_i \tilde{\beta}_1(k_i)/\tilde{S}(k_i) + \sum_{l,m} \tilde{\beta}_2(k_l, k_m)/\tilde{S}(k_l)\tilde{S}(k_m)$ . In the Table 2 we include the cross sections in which this sum was truncated to two terms  $\sigma_1 = \sigma(\tilde{\beta}_0 \oplus \tilde{\beta}_1)$  or to only one term  $\sigma_0 = \sigma(\tilde{\beta}_0)$ . We also present separately the individual contributions from  $\tilde{\beta}_i$ ,  $i = 0, 1, 2$ . All these quantities are calculated in  $O(\alpha^2)$ . The pure  $O(\alpha)$  result  $\sigma' = \sigma(\tilde{\beta}_0 \oplus \tilde{\beta}_1)$  is also included. As a basic measure of the precision of the integrated cross section (from the QED point of view) we take a difference between the first and second order results, i.e., the quantity  $\delta' = (\sigma' - \sigma)/\sigma$ . As we see from the Tables 2 and 3  $|\delta'|$  is below  $1.5 \cdot 10^{-3}$  for  $|\sqrt{s} - M_Z| \leq 2\text{GeV}$  and is below  $5 \cdot 10^{-3}$  far away from the  $Z^0$  peak. We conclude therefore, *rather conservatively*, that from the point of view of the initial state QED bremsstrahlung *the precision of our results for the integrated cross section is better than 0.1% close to the  $Z^0$  peak and 0.5% far away from the  $Z^0$  peak.*

As we see from the Table 2 the series in  $\tilde{\beta}_i$ ,  $i = 0, 1, 2$  (in the second order) converges very rapidly; for instance, the contribution from  $\tilde{\beta}_2$  in the range  $\sqrt{s} = M_Z \pm 2\text{GeV}$  is below 0.02%. It is at most 0.5% far away from the  $Z^0$ . We treat these numbers as a *further confirmation* of the previously stated estimates of the precision. Let us note that even the second order cross section from  $\tilde{\beta}_0$  alone gives near the top of the  $Z^0$  ( $|\sqrt{s} - M_Z| \leq 1\text{GeV}$ ) a very good (better than 1%) estimate of the cross section.

In both Tables 2 and 3 we also demonstrate a remarkable result concerning an agreement of our Monte Carlo cross section with the leading-log type analytical calculation of refs. [3,22]. The second order total cross section is obtained in these works in the leading-log approximation (essentially by convoluting twice the Altarelli-Parisi fragmentation function) and later it is improved by an ad hoc procedure such that the result features a proper soft-photon limit and agrees with the  $O(\alpha)$  exact calculations. There is some freedom in this game and we have exploited it to write a formula of this class which is numerically as close as possible to the result of our Monte Carlo program. We have found that the total cross section given by<sup>(11)</sup>

$$\begin{aligned}\sigma_A &= \int_0^{v_{max}} dv \sigma_{\text{Born}}(s(1-v)) \frac{e^{-C\gamma}}{\Gamma(1+\gamma)} e^{\delta_{\text{YFS}}} \gamma v^{\gamma-1} (1 + \delta_S + \delta_H(v)), \\ \delta_S &= \left(\frac{\alpha}{\pi}\right)(L-1) + \frac{1}{2}\left(\frac{\alpha}{\pi}\right)^2 L^2, \\ \delta_H(v) &= v \left(-1 + \frac{1}{2}v\right) + \left(\frac{\alpha}{\pi}\right)L \left(-\frac{1}{4}(4-6v+3v^2)\ln(1-v) - v\right) \\ L &= \ln \frac{s}{m_e^2}, \quad \gamma = 2\left(\frac{\alpha}{\pi}\right)(L-1), \quad C = 0.57721566\dots,\end{aligned}\tag{6.1}$$

parametrizes the result of our program very well indeed. (See eq. (2.29) for definition of  $\delta_{\text{YFS}}$ .) As we see in Tables 2 and 3 it agrees with the second order Monte Carlo result to within the statistical error which is  $\simeq 0.03\%$  close to the  $Z^0$  and  $\simeq 0.05\%$  away from the  $Z^0$  resonance. Now, the natural question to be asked is: if the Monte Carlo total cross section is reproduced with the above formula so well, then how well does the integrand of the above expression reproduces the Monte Carlo result for the distribution  $d\sigma/dv$ . The interested reader we refer for the answer to Appendix B.

In the Table 2 we also include the best known non-Monte-Carlo result for the second order total cross section of ref. [2]. We show there the full second order calculation without

---

(11) This formula is up to third and higher order corrections equivalent to that presented in ref. [22], although ours is a bit more compact.



fermion pair production and with the by hand “exponentiation”<sup>(12)</sup>. As we see there is a very good, to within 0.1%, agreement of this result with our Monte-Carlo result.

In Figs. 1 and 2 we present the photon multiplicity distribution and the transverse momentum of the muon pair as a whole. All these distributions are produced with samples of more than  $10^5$  events. The photon multiplicity is shown for photons above  $100\text{MeV}$  in a normal situation, without the influence of any resonance, i.e., for  $\sqrt{s} = 40\text{GeV}$ , on the top of  $Z^0$  resonance  $\sqrt{s} = M_Z = 92\text{GeV}$ , where the photon average multiplicity is dampened and at  $\sqrt{s} = 100\text{GeV}$ , in the radiative tail, where it is strongly enhanced. The corresponding average multiplicities are 1.0, 0.75 and 1.52. The distributions of the transverse momentum of the muon pair is shown at the top of the  $Z^0$ . (The analogous distribution off the peak would be more diffuse, for example the average  $p_T$  which is  $0.42\text{GeV}$  at the  $Z^0$  would rise to  $0.88\text{GeV}$  at  $\sqrt{s} = 40\text{GeV}$ . It should be noted that both of these distributions would be also affected by the final state bremsstrahlung significantly.

In the present version of the program all details which do not concern the initial state bremsstrahlung (electroweak corrections, final state bremsstrahlung,  $s$ -dependence of the  $Z^0$  width etc.) are either neglected or included in the simplest form, in order to keep the program and its description maximally simple. All such extensions will be included and discussed in the forthcoming publications [26]. One exception from the above rule is the following numerical example illustrating the effects of the large ultraviolet contributions summed up using technique of the renormalization group. This result may be obtained with a minor modification of the present program, and it addresses the important problem of the interrelation of the soft and ultraviolet divergences in our calculation scheme. More precisely, the result (2.2) and the attendant numerical consequences, as presented until this point, do not address systematically the probable large ultraviolet (UV) logarithms, which may occur in  $\sigma$ . To handle these effects, we have used the Weinberg- ’t Hooft renormalization group [29] to obtain the respective renormalization group improved form of eq. (2.2). The corresponding improvement may be realized by following the recipe in refs. [9,10]. In the following, we wish to illustrate the effects of the improvement.

The following numerical results we have obtained using a version of the present program which was obtained by applying the recipe in refs. [9,10] to eq. (2.2). This rather straightforward modification consists of replacing the QED and weak coupling constants by the corresponding running coupling constants. In particular, the  $SU_{2L}$  charge  $g_W$ , is

---

(12) We would like to thank Gerrit Burgers for providing us the program ZAPPQ for calculating this cross section.

defined at  $M_W$  here, i.e., it is assumed to be close to its value at  $M_W$ . (This is still true even at PEP and PETRA energies.) The other required input is identical to that used before. The corresponding numerical results of this renormalization group improvement are illustrated in Table 4. We see, as we have already realized in refs. [9,10], that at the  $Z^0$  the effect is  $O(1\%)$  and that, away from the  $Z^0$ , it is necessary for the high precision simulations. We see further, however, that the effect of the  $s$ -dependent width, after the fashion of ref. [22], is still observable at the level of 0.1%. This is consistent with the results in ref. [22].

The lesson we draw from this exercise is the following: If one wants the below 1% precision at the  $Z^0$ , the  $s$ -dependent width and the renormalization group improvement should be used; away from the  $Z^0$ , the latter improvement should still be used for such precision.

## 7. Conclusions

The present program represents an example of a successful full implementation of the Yennie-Frautschi-Suura soft photon summation scheme with the help of a powerful Monte Carlo technique. The profit from this approach is three-fold: (1) one may implement an arbitrary set of experimental cut-offs in the calculations (something that was in the original YFS paper discarded as an impossible dream); (2) the perturbative expansion in the number of the noninfrared/hard photons appears to be stable and fast convergent giving rise to high precision results; and (3) there is no need to resort to arbitrary, ad-hoc, "exponentiation" procedures at the very end of the finite order calculations since the proper soft photon resummation is the starting point.

There is a new open perspective of applying the presented techniques to a more difficult case of the final state bremsstrahlung [26] or to the process of Bhabha scattering where it is rather unclear what the usual ad-hoc "exponentiation" procedure would be. We think that in the above more difficult cases the presented technique will allow one to sum up the higher order QED effects very efficiently and the event generators of this class will be a very useful tool in analyzing the experimental data at LEP/SLC. Indeed, the low angle Bhabha scattering event generator employing the presented technique is already available [12]. Let us finally note that the present version of the program including only the initial state radiation will be still useful in many applications (quark pair production) even if a more sophisticated version with the final state bremsstrahlung [26] will become available.

## ACKNOWLEDGEMENTS

The authors are grateful to SLAC and CERN for their hospitality and support, in particular to MARK-II, ALEPH and DELPHI collaborations. The useful discussions and the help in debugging the program from drs. Z. Was and W. de Boer are acknowledged. This work is partly supported by grant no. CPBP.01.09 of the Polish Ministry of Education, by the U.S. Department of Energy, contracts DE-AC03-76SF00515 and DE-AS05-76ER03956, and by a University of Tennessee Faculty Research Award.

## APPENDIX A

### Mellin transform versus Monte Carlo – a relation to YFS notation

In this Appendix we shall show how our master formula (2.2) would look in a standard notation used in ref. [7] and how to translate it from one notation to another. In the notation of ref. [7] the integrated cross section for our process (2.1) reads as follows

$$\begin{aligned} \sigma = & \int \frac{d^4 x}{(2\pi)^4} \int \frac{d^3 q_1}{q_1^0} \frac{d^3 q_2}{q_2^0} \exp[ix(p_1 + p_2 - q_1 - q_2) + D] \exp[2\alpha B + \tilde{B}] \left( \tilde{\beta}_0(\mathcal{R}p_i, \mathcal{R}q_j) \right. \\ & \left. + \int \frac{d^3 k}{k^0} e^{-ixk} \tilde{\beta}_1(\mathcal{R}p_i, \mathcal{R}q_j, k) + \frac{1}{2!} \int \frac{d^3 k_1}{k_1^0} \int \frac{d^3 k_2}{k_2^0} e^{-ixk_1 - ixk_2} \tilde{\beta}_2(\mathcal{R}p_i, \mathcal{R}q_j, k_1, k_2) \right) \end{aligned} \quad (\text{A1})$$

where

$$\begin{aligned} 2\alpha B &= \frac{i\alpha}{4\pi^2} \int \frac{d^4 k}{k^2 - m_\gamma^2} \left( \frac{2p_1 - k}{k^2 - 2p_1 \cdot k} + \frac{2p_2 + k}{k^2 + 2p_2 \cdot k} \right)^2, \\ 2\alpha \tilde{B} &= \int \frac{d^3 k}{k^0} \tilde{S}(p_1, p_2, k) \theta(K_m(\Omega) - k^0), \\ D(p_1, p_2, [K_m]) &= \int \frac{d^3 k}{k^0} \tilde{S}(p_1, p_2, k) \left( e^{-ixk} - \theta(K_m(\Omega) - k^0) \right) \end{aligned} \quad (\text{A2})$$

The function  $\theta(K_m(\Omega) - k^0)$  represents collectively the upper experimental limits on the real photon four-momenta. The advantage of the Monte Carlo is that we may simply put this limit very high, for example, above the phase space limits

$$\theta(K_m(\Omega) - k^0) = \theta(\sqrt{s} - k^0).$$

The integral  $\int d^4 x$  projects out photon four-momenta which do not conserve the total energy-momentum anyway. (The  $x$ -dependent exponent has to be expanded prior to  $x$  integration.) Summarizing, the upper limits on  $k$  integration are provided by the phase space itself and all hard photons are included in the game.

Now comes the second step: we divide the photon energy integration range in  $\tilde{B}$  into  $k^0 < k_\epsilon = \epsilon\sqrt{s}/2$  and  $k^0 > k_\epsilon$ , where the parameter  $\epsilon$  is small (but not necessarily smaller than  $m_e/\sqrt{s}$ )

$$2\alpha\tilde{B} = \int_{k^0 < k_\epsilon} \frac{d^3k}{k^0} \tilde{S}(k) + \int_{k^0 > k_\epsilon} \frac{d^3k}{k^0} \tilde{S}(k) \theta(\sqrt{s} - k^0) = \tilde{B}(\epsilon) + R(\epsilon) \quad (\text{A3})$$

We combine then  $R(\epsilon)$  with  $D$  and we obtain

$$D' = D + R(\epsilon) = \int_{k^0 < k_\epsilon} \frac{d^3k}{k^0} \tilde{S}(k) (e^{-ixk} - 1) + \int_{k^0 > k_\epsilon} \frac{d^3k}{k^0} \tilde{S}(k) e^{-ixk} \theta(\sqrt{s} - k^0) \quad (\text{A4})$$

Now we observe that the first integral in the above formula vanishes in the limit  $\epsilon \rightarrow 0$  and furthermore the  $\theta(\sqrt{s} - k^0)$  factor in the second integral can be omitted because  $\int d^4x$  provides an even stronger cut-off. Taking this into account we obtain

$$\begin{aligned} \sigma = \int \frac{d^4x}{(2\pi)^4} \int \frac{d^3q_1}{q_1^0} \frac{d^3q_2}{q_2^0} \exp \left[ ix(p_1 + p_2 - q_1 - q_2) + \int_{k^0 > k_\epsilon} \frac{d^3k}{k^0} e^{-ixk} \tilde{S}(k) \right] \\ \exp \left[ 2\alpha B + \tilde{B}(\epsilon) \right] \left( \tilde{\beta}_0(\mathcal{R}p_i, \mathcal{R}q_j) + \int \frac{d^3k}{k^0} e^{-ixk} \tilde{\beta}_1(\mathcal{R}p_i, \mathcal{R}q_j, k) + \dots \right). \end{aligned} \quad (\text{A5})$$

It is now enough to expand the  $x$ -dependent exponent and to integrate over  $x$  in order to obtain our master formula (2.2).

What are the most important differences between the Yennie-Frautschi-Suura formula (A1) and our master formula (2.2)? The first is manifestly infrared finite but it cannot be used directly for the Monte Carlo. The second is well suited for Monte Carlo integration, it apparently depends on infrared cut-off  $\epsilon$  but, in fact,  $\epsilon$  is a dummy regulator and it can be proved that in the limit  $\epsilon \rightarrow 0$  none of the physically meaningful results depend on it. The independence of the total cross section can be shown either by reintroducing the Mellin transform and going back to Y-F-S formulation or by simple algebraic calculation – without resorting to the Mellin transform, or even finally by differentiating eq. (2.2) with respect to  $\epsilon$ . In fact the expression (A1) is as a generating functional for eq. (2.2). What should be strongly stressed, however, is that both formulations are *totally equivalent*.

From the eq. (A1) it is also rather clear that the reduction operation  $\mathcal{R}$  may depend on the fermion momenta  $p_i, q_i$  but it in no way depends on the momenta of the individual photons. If this were not true then the equivalence between the eq. (2.2) and the eq. (A1) would have been broken and even the infrared finiteness would have been threatened.

## APPENDIX B

### More on Monte Carlo weights – the $v$ distribution

The aim of this Appendix is to answer the question: is it possible in the Monte Carlo program of the type presented here, which calculates numerically a complicated multidimensional integral with the precision below 0.1%, to understand in a fine detail how the final numerical result is built up. As we have indicated already in Sections 2 and 6 one should look for the answer in the distribution of the variable  $v$

$$\frac{d\sigma}{dv} = \frac{d\sigma_{\text{crude}}}{dv} < \prod_{i=1}^4 w_i >_{\text{crude}}, \quad \frac{d\sigma_{\text{crude}}}{dv} = e^{\delta_{\text{YFS}}} \gamma v^{\gamma-1} \mathcal{J}_0(v) E_{\text{mass}}(v) \sigma_{\text{Born}}(s(1-v)), \quad (\text{B1})$$

where the average  $< \dots >_{\text{crude}}$  is taken over the Monte Carlo events generated according to  $d\sigma_{\text{crude}}$ . We shall show that in the above distribution it is possible to understand qualitatively and quantitatively the magnitude and the  $v$ -dependence of the various components and therefore the magnitude of the Monte Carlo total cross section as well. Many of the quantities discussed in this Appendix may be found in the output of the program and we shall indicate where to find them and what values are expected. To obtain some of them it is necessary to run the program for fixed  $v$ . This is not a normal mode of work and we refer the interested user to the comments in the program on the necessary arrangement of the input parameters.

For the purpose of our detailed weight-analysis it is convenient to rewrite the eqs. (B1) as follows

$$\begin{aligned} \frac{d\sigma}{dv} &= \frac{d\sigma_{\text{ref}}}{dv} < f_1 f_2 f_3 f_4 >_{\text{ref}}, \quad \frac{d\sigma_{\text{ref}}}{dv} = \gamma v^{\gamma-1} \sigma_{\text{Born}}(s(1-v)), \\ f_1 &= w_1 E_{\text{mass}}(v), \quad f_2 = w_2 \mathcal{J}_0(v), \quad f_3 = w_3, \quad f_4 = w_4 e^{\delta_{\text{YFS}}}. \end{aligned} \quad (\text{B2})$$

It should be noted that for fixed  $v$  there is no difference between the two averages  $< \dots >_{\text{crude}}$  and  $< \dots >_{\text{ref}}$ . In the following we shall look into the average weights  $< f_i >_{\text{ref}}$ ,  $i = 1, 2, 3$  separately, then into  $< f_1 f_3 >_{\text{ref}}$  and  $< f_1 f_2 f_3 >_{\text{ref}}$ , and finally we shall include the model weight  $f_4$  into the game. It makes sense to explore the average weights separately because, as we shall see, a simple factorization principle  $< f_1 f_2 f_3 >_{\text{ref}} = < f_2 >_{\text{ref}} < f_1 f_3 >_{\text{ref}}$  holds. Let us note that the *reference* differential cross section  $d\sigma_{\text{ref}}/dv$  which we have isolated out, when taken alone, determines the value of the total cross section to within 10%. Furthermore, for the  $\sigma_{\text{Born}}$  weakly dependent on  $s$  we have roughly  $\sigma_{\text{ref}} \simeq \sigma_{\text{Born}}(s)$  due to  $\int_0^1 \gamma v^{\gamma-1} dv = 1$ . In order to see better what happens in the case of the production of the  $Z^0$  resonance we shall typically “expand” the region of the small  $v$  (which contributes

most of the total cross section) by introduction of a convenient “natural” variable  $z = v^\gamma$  in which  $d\sigma_{\text{ref}}/dz \simeq \sigma_{\text{Born}}(s(1 - z^{1/\gamma}))$ . This new distribution turns out to be rather flat for  $z < 0.5$  and may show up a resonance structure above  $z \simeq 0.5$ . The value of  $\sigma_{\text{Born}}$  changes less than 1% for  $z < 0.57$  ( $v < 5.4 \cdot 10^{-3}$ ) at  $\sqrt{s} = M_Z$ , for  $z < 0.53$  ( $v < 2.8 \cdot 10^{-3}$ ) at  $\sqrt{s} = M_Z + 2\text{GeV}$  and for  $z < 0.39$  ( $v < 1.6 \cdot 10^{-4}$ ) at  $\sqrt{s} = M_Z - 2\text{GeV}$ .

The factor  $E_{\text{mass}}(v)$ , as it was pointed out in Section 2, is canceled exactly by the *mass* weight  $w_2$ , i.e., we expect  $\langle f_1 \rangle_{\text{ref}} \equiv 1$ . All that is a purely technical trick – we overpopulate the region of the phase space with photons almost collinear to  $e^\pm$  in order to reject these supplementary events shortly after. Not quite all of them are rejected however – the *model* weight  $w_4$  spares some of them from the rejection. This is related to the fact that soft photons cannot flip fermion helicity while hard photons can. The corresponding additional helicity-flip (positive) contribution to the differential cross section is located almost entirely in the region of the very small angle photon emission, see ref. [30]. If we did not take this phenomenon into account in the  $d\sigma_{\text{crude}}$ , the total Monte Carlo rejection weight would fluctuate wildly (although for a small fraction of events), threatening the overall convergence of the calculation. The quantity  $\langle f_1 \rangle_{\text{ref}} - 1$  is calculated in the program and printed in the window B, position B0 of the output from the routine KARLUD. The user of the program may verify by himself that within a statistical error this quantity is always equal to zero.

The weight

$$f_2 = \mathcal{J}_0(v)w_2 = \mathcal{J}(\bar{K}, v) = \frac{1}{2} \left( 1 + \frac{1}{\sqrt{1 - Av}} \right) \quad (\text{B3})$$

includes the variable  $A = K^2 P^2 / (KP)^2$  which is a (complicated) function of the total photon momentum  $K$  such that  $0 \leq A \leq 1$  and for small effective mass  $K^2$  of the photon system  $A \simeq 0$ . The origin of the above weight is related to the rescaling transformation used to impose the energy conservation on the photons. The presence of the weight  $f_2$  reflects the fact that this dilatation transformation underpopulates the region of the phase space with the two hard anticollinear photons. In the Monte Carlo  $f_2$  is introduced in such a way that first we overpopulate all hard photon events by inclusion of  $\mathcal{J}_0(v)$  in the  $d\sigma_{\text{crude}}$  and later on we reject selectively with the weight  $w_2$  giving more survival chances to events with antiparallel photons. The factor  $\mathcal{J}_0(v)$  from  $d\sigma_{\text{crude}}$  cancels precisely the other factor  $\mathcal{J}_0^{-1}(v)$  in  $w_2$ , leaving in the  $d\sigma/dv$  the net result  $f_2$ . The program provides an information on  $\langle f_2 \rangle_{\text{ref}}$ : in the window B position B2, of the output from routine KARLUD one may find the Monte Carlo result for  $\langle f_2 \rangle_{\text{ref}}$ . From the inspection of the eq. (B3) we expect  $\langle f_2 \rangle_{\text{crude}} \simeq 1$  for  $v \ll 1$ . The Monte Carlo calculation gives  $1 \leq \langle f_2 \rangle_{\text{ref}} \leq 1.001$  for

$v < 0.03$  and it increases up to  $\langle f_2 \rangle_{\text{crude}} \simeq 1.06$  for  $v \simeq 0.9$ . The Monte Carlo result for this average is plotted as a function of  $z = v^\gamma$  in Fig. 3a.

The third weight  $f_3 = w_3$  is related again to the process of imposing the energy conservation on the photons by means of the scaling down of the photon momenta. In this procedure we get sometimes an event with the energy below the  $\epsilon\sqrt{s}/2$  limit. Such an event is attributed the zero weight and is later rejected. The weight  $f_3$  is a complicated function of the photon momenta; nevertheless, we know almost everything about its average. First of all, in the range  $\epsilon \ll v \ll 1$  we expect

$$\langle f_3 \rangle_{\text{ref}} = \frac{e^{-C\gamma'}}{\Gamma(1 + \gamma')} = g(\gamma') \quad (\text{B4})$$

and/or equivalently

$$\langle f_3 f_1 \rangle_{\text{ref}} = \frac{e^{-C\gamma}}{\Gamma(1 + \gamma)} = g(\gamma). \quad (\text{B5})$$

These identities are related to the well known phenomenon of the competition of the soft photons for the total energy. The right hand side of eq. (B5) is the result of the analytical calculation made with the help of the Mellin transform, see for instance refs. [7,13]. From the Monte Carlo calculation this average (probably for the first time) was obtained in ref. [8]. The value of  $\langle f_3 f_1 \rangle_{\text{ref}} - g(\gamma)$  is included in the output of the program, see window B, entry B8, of the output from KARLUD, and one may see that for  $10^2\epsilon \leq v < 0.2$  it is equal zero to within  $10^{-3}$ . What about lower values of  $v$ ? First of all  $f_2 \equiv 1$  for  $v \leq \epsilon$ , on the other hand, again from the analytical calculation [7], it is known that

$$\int_{0 \leq v \leq v_{\text{max}}} w_1 w_3 d\sigma_{\text{crude}} \simeq \int_{0 \leq v \leq v_{\text{max}}} f_1 f_3 d\sigma_{\text{ref}} = v_{\text{max}}^\gamma \frac{e^{-C\gamma}}{\Gamma(1 + \gamma)} \sigma_{\text{Born}}(s). \quad (\text{B6})$$

This relation will be true provided that  $\epsilon \ll v_{\text{max}} \ll 1$  and  $v_{\text{max}}$  is small enough for  $\sigma_{\text{Born}}(s(1-v))$  to be independent of  $v$ . The above identity implies that the average  $\langle f_1 f_3 \rangle$  has to have some structure near  $v = \epsilon$ . One can make a Monte Carlo numerical exercise and plot  $\langle f_1 f_3 \rangle_{\text{ref}}$  as a function of  $z = v^\gamma$ . As we see in Fig. 3a,  $\langle f_1 f_3 \rangle_{\text{ref}} \equiv 1$  for  $v \leq \epsilon$ , then  $\langle f_1 f_3 \rangle_{\text{ref}} \simeq g(\gamma)$  for  $10^2\epsilon < v$  and, finally, in the region  $\epsilon < v < 10^2\epsilon$  it shows a few percent dip. Since our program reproduces eq. (B6) rather well it is therefore quite obvious that the role of the dip is to correct the integrated cross section for the lack of the factor  $g(\gamma)$  in the  $0 < v < \epsilon$  range. The net influence of the above unphysical structure on the integrated cross section and other observables is in the limit  $\epsilon \rightarrow 0$  totally negligible

and we may really not worry about it. The only practical lesson is that *the cut-off  $\epsilon$  should be kept about a factor of  $10^2$  below the resolution limit* set by the experiment or the energy variation of  $\sigma_{\text{Born}}$ .<sup>(13)</sup> The mechanism of the dip development is rather simple: Contrary to the situation in the region  $v_{\text{max}} \gg \epsilon$  where the frequency of an event with the photon energy falling below the  $\epsilon\sqrt{s}/2$  limit is independent of  $v$  and equals precisely  $1 - g(\gamma)$ , for  $v$  approaching  $\epsilon$  such an event happens more often. This is true for events with two or more photons. For example the two photons with the energy above  $\epsilon\sqrt{s}/2$  cannot make  $v$  below  $2\epsilon$ , i.e., all events with  $\epsilon < v < 2\epsilon$  and the photon multiplicity  $n \geq 2$  will get rejected. (This well known phenomenon can be observed already in the conventional second order QED calculation.)

The collective result  $\langle f \rangle = \langle f_1 f_2 f_3 \rangle_{\text{ref}}$  is plotted in Fig. 3b as a function of  $z$ . As we see, from comparing Figs. 3a and 3b the factorization  $\langle f \rangle = \langle f_2 \rangle \langle f_2 f_3 \rangle$  holds, the  $v$  dependence of  $\langle f \rangle$  is now fully understood and can be summarized as follows: The dip in the vicinity of  $v = \epsilon$  and the plateau  $\langle f \rangle \equiv 1$  for  $v < \epsilon$  are the unphysical artifacts of the Monte Carlo integration with the finite cut-off (infrared regulator)  $\epsilon$  while the  $\langle f \rangle = g(\gamma)$  plateau for  $v > 10^2 \epsilon$  is the “normal” situation and the slight enhancement of  $\langle f \rangle$  at higher  $v$  reflects the phase space factor  $f_2$  from hard anticollinear photons. The net effect of the weights  $f_i$ ,  $i = 1, 2, 3$  can be summarized in the effective distribution which for  $v < 10^{-2}$  approximates well the Monte Carlo result

$$\left( \frac{d\sigma_{\text{ref}}}{dv} \langle f_1 f_2 f_3 \rangle_{\text{ref}} \right)_{\text{eff.}} = \gamma v^{\gamma-1} \frac{e^{-C\gamma}}{\Gamma(1+\gamma)} \sigma_{\text{Born}}(s(1-v)). \quad (\text{B7})$$

This looks already like a part of the integrand in eq. (6.1). Let us include now the model weight  $f_4 = e^{\delta_{\text{VFS}}} w_4$  in the game. It includes the sum of the contributions from  $\tilde{\beta}_0$ ,  $\tilde{\beta}_1$  and  $\tilde{\beta}_2$ . As it was indicated in Section 6 the magnitude of the corresponding contribution is provided by the program. From a series of the MC events generated at various fixed  $v$ 's one may learn that for  $v < 10^{-3}$  the contribution from  $\tilde{\beta}_0$  dominates, i.e., the relative contribution from the other two  $\tilde{\beta}$ 's is below  $10^{-3}$ . (In fact  $\tilde{\beta}_2$  switches on, at the same level of  $10^{-3}$ , for much higher  $v$ , i.e., for  $v > 0.12$ .) The net contribution from  $\tilde{\beta}_0$  will be roughly  $1 + \delta_S$  where  $\delta_S = (\alpha/\pi)(L-1) + \frac{1}{2}(\alpha/\pi)^2 L^2$ , see the second order expression for  $\tilde{\beta}_0$  in eq. (3.1). The main role of the contribution from  $\tilde{\beta}_1$  is to reinstall in the spin factor

---

(13) Let us note that if we had lowered  $\epsilon$  then the dip would move gradually to  $z = 0$  and, for extremely low  $\epsilon$ , it would disappear completely. Such a small  $\epsilon$  would be rather inconvenient, however, due to unnecessary loss of the speed of the program.



$\frac{1}{2}(1 + (1 - v)^2)$  in  $d\sigma/dv$ . In view of that it is quite clear that the Monte Carlo result for  $d\sigma/dv$  can be parametrized with an effective distribution

$$\left(\frac{d\sigma}{dv}\right)_{eff.} = e^{\delta_{YFS}} \gamma v^{\gamma-1} \frac{e^{-C\gamma}}{\Gamma(1+\gamma)} (1 + \delta_S) \frac{1 + (1 - v)^2}{2} \sigma_{Born}(s(1 - v)). \quad (B8)$$

In the next plot, see Fig. 4, we shall compare the complete second order Monte Carlo (MC) results for  $d\sigma/dz$  with the other Monte Carlo and analytical results. In order to be able to see the effects at the “resolution” level of 0.1% we have to remove from  $d\sigma/dz$  large and “trivial” effects discussed above, see eq. (B8). All fine details can be seen if we look into the distribution

$$\rho(z) = \frac{d\sigma/dv}{\gamma v^{\gamma-1} \sigma_{Born}(s(1 - v)) \frac{1}{2}(1 + (1 - v)^2)} = \frac{d\sigma/dz}{\sigma_{Born}(s(1 - z^{1/\gamma}))(1 + (1 - z^{1/\gamma})^2)/2} \quad (B9)$$

In Fig. 4 we plot the MC first and second order result for  $\rho(z)$ , all from the MC runs at fixed  $v$ . The MC results below  $v = 0.01$  are consistent with the previously discussed  $z$ -dependence of the average  $\langle f \rangle = \langle f_1 f_2 f_3 \rangle_{ref.}$ . The second order MC result agrees well with the formula (6.1) – the biggest difference being 0.5% at  $v = 0.9$ . It is therefore not surprising that the corresponding total cross sections near  $Z^0$  resonance agree to within 0.03%, see Table 2. The first and second order MC results start to differ for  $v > 0.2$  and the difference goes up to 12% for  $v = 0.8$ . In the plot we have also included the typical example of the first order analytical “exponentiated” result of ref. [3]; more precisely it is a version of ref. [22] with the truncated second order terms. It differs with all other MC and analytical results at the level of a few percent for  $v > 0.5$ . It is interesting to observe that the MC first order result at  $v > 0.4$  tends to underestimate the differential cross section. It is related to the fact that the  $\tilde{\beta}_1$  contribution in this region is negative and, since  $\tilde{\beta}_2$  is not included, the events with two hard photons contribute roughly twice the contribution from  $\tilde{\beta}_1$ . This sort of double counting is corrected by inclusion of  $\tilde{\beta}_2$  in the second order. The first order analytical “exponentiation” shows an opposite tendency of overestimating the differential cross section in the same high  $v$  region.

What is the precision of the distribution  $d\sigma/dv$  obtained from our program from the point of view of the higher order QED corrections? From the smallness of the  $\tilde{\beta}_1$  and  $\tilde{\beta}_2$  contribution we deduce that for  $v < 0.2$  it is better than 0.1%. In ref. [16] it was found<sup>(14)</sup>

---

(14) This result was obtained by solving, up to infinite order (numerically), the Lipatov evolution equation for the nonsinglet structure function of the electron.

that the influence of the third and higher orders in the region  $0.2 < v < 0.8$  is below 0.5% level. This is consistent with the difference between the second order MC result and the analytical result of eq. (6.1), as may be seen in Fig. 4, and we treat this as an estimate of the precision.

Summarizing, the above detailed weight analysis shows that the total cross section consists of a few simple building blocks. We are able to understand qualitatively and quantitatively the  $v$ -behavior and the magnitude of the each component and, therefore, of the total cross section as well.

**Table 1**

The alphabetic list of the important and frequently used variables.

Variable	Common	Description
ALF1	----	$\alpha/\pi$
ALFINV	----	$1/\alpha$ , the inverse of the QED coupling constant
AMFIN	WEKING	$m_f$ , mass of the final fermion
AMEL	WEKING	$m_e$ , electron mass
AMAZ	WEKING	$M_Z$ , mass of the $Z^0$
BETA0	----	$\tilde{\beta}_0$ second order result
BET1D	----	$\tilde{\beta}_1(k_l)/\tilde{S}(k_l)$ second order result
BET2D	----	$\tilde{\beta}_2(k_l, k_m)/\tilde{S}(k_l)\tilde{S}(k_m)$ second order result
BET1DX	----	$\tilde{\beta}_1(k_l)/\tilde{S}(k_l)$ first order result
BETA0X	----	$\tilde{\beta}_0$ first order result
BETI	VVREC	$\gamma = 2(\alpha/\pi)(\ln s/m_e^2 - 1)$
CMSENE	----	center of the mass energy, $\sqrt{s}$
DISCRU	----	$b_0$ crude Monte Carlo distribution
DJAC	----	$\mathcal{J}(\bar{K}, v)$ , dilatation Jacobian
ENE	WEKING	beam energy, $\sqrt{s}/2$
EXPY	----	$1/\lambda_0(\bar{K}, v)$ , dilatation factor
GAMMZ	WEKING	$\Gamma_Z$ , width of the $Z^0$
IDF	WEKING	final fermion identifier, IDF=2,3,4 for $\mu, u, d$
KEYRAD	KEYYFS	=3,2 radiation switch for second, first order calculation
NOUT	----	output unit number, set in routine EXPAND
NPHOT	MOMSET	$n$ , photon multiplicity
PI	----	$\pi$
QF1,QF2	MOMSET	$q_{1,2}$ , final fermion four momenta, GeV
SPHOT	MOMSET	list of photon four-momenta, GeV
SPHUM	MOMSET	sum of photon four-momenta, GeV
SINW2	WEKING	$\sin^2 \theta_W$ , $\theta_W$ is the electroweak mixing angle
SVAR	----	$s$
SVAR1	----	$s' = s(1 - v)$ , mass of final fermion pair squared
VV	VVREC	$v = 1 - s'/s$
VVMIN	VVREC	$\epsilon$ , infrared cut-off
VVMAX	VVREC	$v_{max}$ , upper limit for $v$
WT1,2,...	----	$w_1, w_2, \dots$ weights

**Table 2**

Table of the cross sections for the muon pair production process. The following parameters were used:  $M_Z = 92\text{GeV}$ ,  $\Gamma_Z = 2.45346$ ,  $\sin^2 \theta_W = 0.228818$ . An upper limit on the photon phase space was  $v_{max} = 0.8$  and the infrared cutoff  $\epsilon = 10^{-6}$ . The A6,B1 etc. indicate a line in one of the three windows in the output from subprogram EXPAND, where the corresponding quantities may be read out. All cross sections are in units of  $\sigma_p = 4\pi\alpha^2/3s$  (so called R-units). The cross section  $\sigma_E$  is the best available non-Monte-Carlo result from ref. [2]; we show their "exponentiated" second order result, with the omission of the production of additional fermion pairs.

$\sqrt{s}$ , cms energy	92GeV	94GeV	90GeV
A6: No. of events	$4.0 \cdot 10^5$	$3.1 \cdot 10^5$	$3.9 \cdot 10^5$
A0: $\sigma = \sigma(\tilde{\beta}_0 \oplus \tilde{\beta}_1 \oplus \tilde{\beta}_2)$ , $O(\alpha^2)$	$131.53 \pm 0.04$	$58.37 \pm 0.02$	$33.65 \pm 0.01$
B1: $\sigma_1 = \sigma(\tilde{\beta}_0 \oplus \tilde{\beta}_1)$ , $O(\alpha^2)$	$131.52 \pm 0.04$	$58.37 \pm 0.02$	$33.64 \pm 0.01$
B0: $\sigma_0 = \sigma(\tilde{\beta}_0)$ , $O(\alpha^2)$	$132.16 \pm 0.03$	$59.44 \pm 0.02$	$33.94 \pm 0.01$
B4: $\delta_2 = \frac{\sigma - \sigma_1}{\sigma}$ , contr. from $\tilde{\beta}_2$	$(0.65 \pm .02)10^{-4}$	$(1.73 \pm .04)10^{-4}$	$(2.23 \pm .04)10^{-4}$
B3: $\delta_1 = \frac{\sigma_1 - \sigma_0}{\sigma}$ , contr. from $\tilde{\beta}_1$	$(-4.91 \pm .06)10^{-3}$	$(-18.40 \pm .04)10^{-3}$	$(-8.85 \pm .05)10^{-3}$
B5: $\sigma' = \sigma(\tilde{\beta}_0 \oplus \tilde{\beta}_1)$ , $O(\alpha^1)$	$131.34 \pm 0.04$	$58.30 \pm 0.02$	$33.60 \pm 0.01$
$\delta' = \frac{\sigma' - \sigma}{\sigma}$ ,	$(-1.5 \pm .3)10^{-3}$	$(-1.3 \pm .4)10^{-3}$	$(-1.5 \pm .4)10^{-3}$
C8: $\sigma_A$ , analyt. result eq. (6.1)	131.55	58.38	33.64
C9: $\delta_A = (\sigma_A - \sigma)/\sigma$	$(-0.2 \pm .3)10^{-3}$	$(0.2 \pm .4)10^{-3}$	$(0.1 \pm .4)10^{-3}$
$\sigma_E$ , Berends et. al. [2], $O(\alpha^2)$	131.64	58.46	33.67
$\sigma'_E$ , Berends et. al. [2], $O(\alpha^1)$	132.03	58.38	33.76
$\delta_E = (\sigma_E - \sigma)/\sigma$	$(0.8 \pm .3)10^{-3}$	$(1.4 \pm .4)10^{-3}$	$(0.6 \pm .4)10^{-3}$

**Table 3**

Selected quantities of the Table 2, with the same input parameters, but for a wider range of energy. The cross section is again in R-units.

$\sqrt{s}$ [GeV]	$\sigma$	$\delta_2 \cdot 10^3$	$\delta' \cdot 10^3$	$\delta_A \cdot 10^3$	$\delta_E \cdot 10^3$
40	$1.1026 \pm 0.0006$	$5.11 \pm .03$	$-4.8 \pm .5$	$0.5 \pm .5$	$-0.3 \pm .5$
90	$33.65 \pm 0.01$	$0.22 \pm 0.01$	$-1.5 \pm 0.4$	$0.1 \pm 0.3$	$0.6 \pm 0.4$
91	$73.33 \pm 0.02$	$0.10 \pm 0.03$	$-1.5 \pm 0.3$	$0.0 \pm 0.3$	$0.6 \pm 0.3$
92	$131.53 \pm 0.04$	$0.065 \pm 0.002$	$-1.5 \pm 0.3$	$0.0 \pm 0.3$	$0.8 \pm 0.3$
93	$93.38 \pm 0.03$	$0.088 \pm 0.002$	$-1.4 \pm 0.3$	$0.1 \pm 0.3$	$0.7 \pm 0.3$
94	$58.38 \pm 0.02$	$0.174 \pm 0.004$	$-1.3 \pm 0.4$	$-0.2 \pm 0.4$	$1.4 \pm 0.4$
100	$13.21 \pm 0.01$	$1.56 \pm 0.01$	$-0.8 \pm 0.7$	$0.8 \pm 0.8$	$0.6 \pm 0.7$

**Table 4**

The cross section as in Table 2, with the same input parameters: (a), including the effects of renormalization group improvement and the  $s$ -dependent width; and (b), including only the effect of the  $s$ -dependent width. The cross section is again in R-units.

$\sqrt{s}$ [GeV]	$\sigma(a)$	$\sigma(b)$
40	$1.2198 \pm 0.0005$	$1.1024 \pm 0.0004$
90	$38.17 \pm 0.01$	$34.40 \pm 0.01$
91	$80.10 \pm 0.02$	$75.21 \pm 0.02$
92	$133.48 \pm 0.03$	$132.04 \pm 0.03$
93	$102.24 \pm 0.03$	$97.56 \pm 0.02$
94	$62.05 \pm 0.02$	$57.39 \pm 0.02$
100	$14.407 \pm 0.008$	$13.134 \pm 0.008$

## REFERENCES

1. S. L. Glashow, Nucl. Phys. **22** (1961) 579;  
S. Weinberg, Phys. Rev. Lett. **19** (1967) 1264; Phys. Rev. **D5** (1972) 1412;  
A. Salam, in *Elementary Particle Theory*, ed. N. Svartholm, Stockholm, 1968, p  
361.
2. F. A. Berends and W. L. Van Neerven and G. J. H. Burgers, Nucl. Phys. **B297**  
(1988) 249.
3. E. A. Kuraiev and V. S. Fadin, Sov. J. Nucl. Phys. **41** (1985) 466
4. G. Altarelli and G. Martinelli in, "Physics at LEP", ed. J. Ellis and R. Peccei, CERN  
Report 86-02, vol. 1, p. 47.
5. J. P. Alexander, G. Bonvicini, P. S. Drell and R. Frey, "Radiative Corrections to the  
 $Z^0$  resonance", SLAC-PUB-4376, Phys. Rev. **D37** (1988) 56.
6. F. A. Berends, R. Kleiss and S. Jadach, Comp. Phys. Commun. **29** (1983) 185.
7. D. R. Yennie, S. C. Frautschi and H. Suura, Annals of Phys. **13** (1961) 379.
8. S. Jadach, "Yennie-Frautschi-Suura soft photons in the Monte Carlo generators",  
preprint of Max-Planck-Institut, München, MPI-PAE/PTh 6/87 (1987).
9. S. Jadach and B. F. L. Ward, SLAC-PUB-4543 (1988), Phys. Rev. **D38** (1988)  
2897.
10. B. F. L. Ward, Phys. Rev. **D36** (1987) 939; Acta Phys. Pol. **B19** (1988) 465.
11. S. Jadach, Z. Wąs, R. G. S. Stuart and B. F. L. Ward, "KORALZ: a Monte Carlo  
program for  $\tau$  and  $\mu$  pair production processes at LEP/SLC", unpublished, may be  
obtained from Z. Wąs: ZBW @ DM0MPI11.
12. S. Jadach and B. F. L. Ward, "BIHLUMI: a multiphoton Monte Carlo for Bhabha  
scattering at low angles", unpublished, may be obtained from B.F.L. Ward: BFLW  
@ SLACVM.
13. M. Greco, G. Pancheri and Y. N. Srivastava, Nucl. Phys. **B101** (1975) 234;  
Phys. Lett. **56B** (1975) 367.
14. K. T. Mahanthappa, Phys. Rev. **126** (329) 1962.
15. S. Jadach, Comp. Phys. Commun. **9** (1975) 273.
16. S. Jadach and M. Skrzypek, Jagellonian University preprint TPJU-3/89, January  
1989.

17. F. A. Berends and R. Kleiss, Nucl. Phys. **B177** (1981) 237.
18. G. Altarelli and G. Parisi, Nucl. Phys. **B126** (1977) 298.
19. CALKUL Collaboration, Phys. Lett. **105B** (1981) 215, **114B** (1982) 203; Nucl. Phys. **B206** (1982) 53, **B206** (1982) 61, **B239** (1984) 382, **B239** (1984) 395.
20. G. Marsaglia and A. Zaman, Florida State Univ. report FSU-SCRI-87-50, (1987).
21. S. Jadach, J.H. Kühn, R.G. Stuart and Z. Wąs, Z. Phys. **C38** (1988) 609.
22. G. Burgers, "The shape and size of the  $Z$  resonance", in "Polarization at LEP", CERN report 88-06, eds. J. Ellis and R. Peccei, CERN, Geneva, (1988).
23. B.A. Kniehl, M. Krawczyk, J.H. Kühn and R.G. Stuart, MPI-PAE/PTh 93/87, MPI-München (1988) preprint and in "Polarization at LEP", CERN report 88-06, eds. J. Ellis and R. Peccei, CERN, Geneva, (1988).
24. D. C. Kennedy, B. W. Lynn, C. J.-C. Im and R. G. Stuart, "Electroweak Cross Sections and Asymmetries at the  $Z^0$ ", SLAC-PUB-4128, 1988.
25. S. Jadach and Z. Wąs, "Suppression of QED interference contributions to the charge asymmetry at the  $Z^0$  resonance", CERN-TH.5127/88 preprint (1988), to appear in Phys. Lett. **B**.
26. "YFS3.x Monte Carlo ...", S. Jadach, B.F.L. Ward and Z. Wąs, in preparation.
27. S. Jadach and Z. Wąs, "Systematic uncertainties in the measurement of  $A_{pol}$  with  $\tau$  pairs" in "Physics at LEP", CERN report 86-2, eds. J. Ellis and R. Peccei, CERN, Geneva, (1986).
28. F. Boillot and Z. Wąs, "Uncertainties in the  $\tau$  polarization measurement in LEP-/SLC", preprint of MPI-München, MPI-PAE/Exp El.196/88 (1988), Zeits. Phys. **C** in press.
29. S. Weinberg, Phys. Rev. **D8** (1973) 3497; G. 't Hooft, Nucl. Phys. **B61** (1973) 455.
30. Z. Wąs, Acta Phys. Pol. **B18** (1987) 1099.

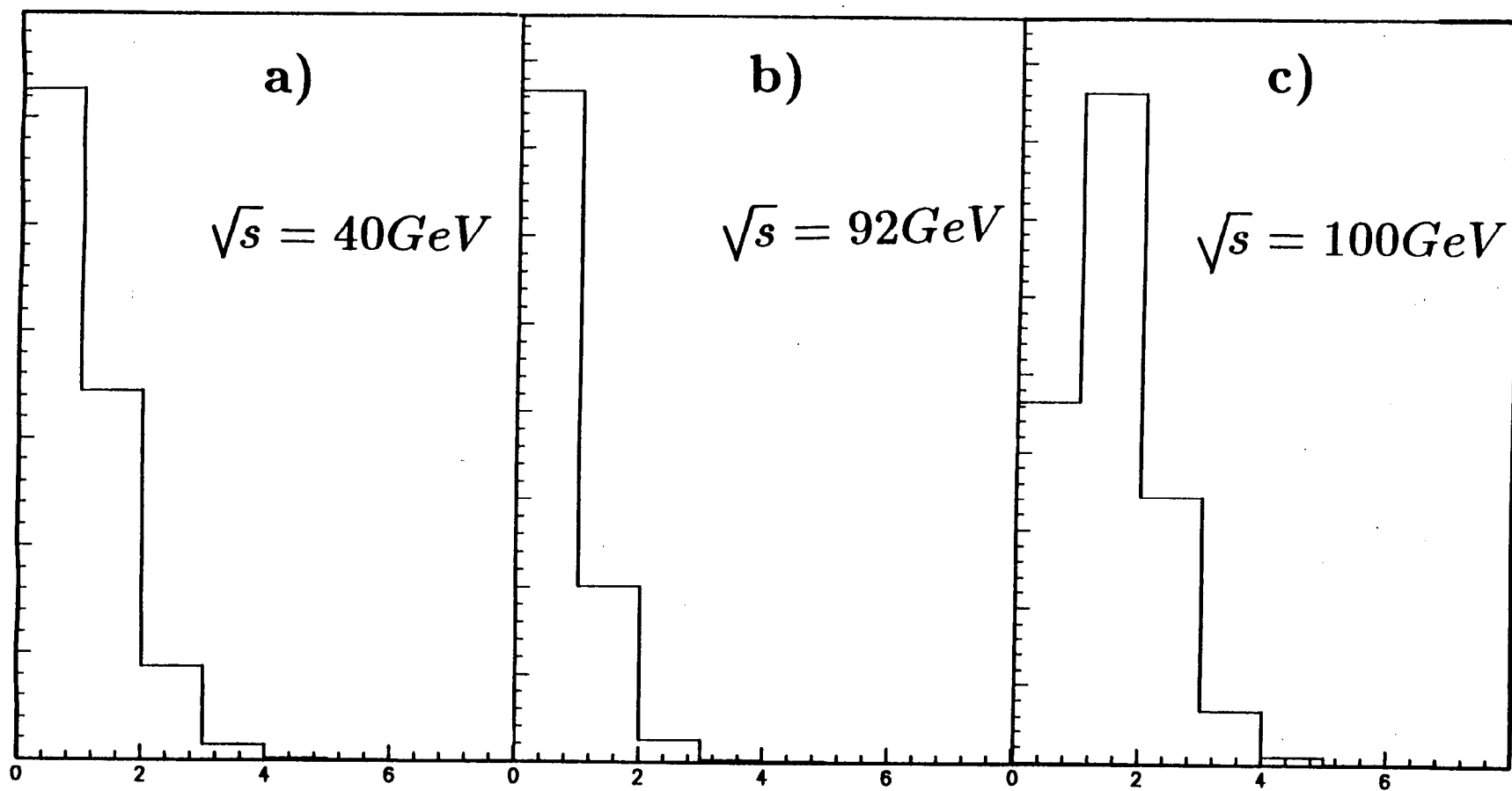


## FIGURE CAPTIONS

1. The photon multiplicity distribution for photons with the energy above 100MeV. The center of the mass energy is  $\sqrt{s}$  is: a) 40GeV, b) 92GeV, c) 100GeV. The Monte Carlo samples include more than  $10^5$  events. The distributions are normalized in an arbitrary units.
2. The transverse momentum distribution of the final state muon pair. The center of the mass energy is  $\sqrt{s}$  is 92GeV. The Monte Carlo sample includes about  $4 \cdot 10^5$  events. The distributions is normalized in the number of the events.
3. The Monte Carlo results for the various internal weights: a) triangles and dots represent  $\langle f_2 \rangle_{\text{ref}}$  and  $\langle f_1 f_2 \rangle_{\text{ref}}$  correspondingly, b) dots denote  $\langle f \rangle = \langle f_1 f_2 f_3 \rangle_{\text{ref}}$ , all as a function of  $z = v^\gamma$ . The  $v$  scale is also marked. The statistical errors are less then the size of dots/triangles. The dashed line marks  $g(\gamma) = e^{-C\gamma}/\Gamma(1 + \gamma)$ . This plot is essentially almost independent of  $\sqrt{s}$ . In the calculations we have used  $\sqrt{s} = M_Z = 92\text{GeV}$  and  $\epsilon = 10^{-6}$ .
4. The plot of the  $\rho(z) = (2d\sigma/dz) / (\sigma_{\text{Born}}(s(1 - z^{1/\gamma}))(1 + (1 - z^{1/\gamma})^2))$ . Dots and squares represent the second and first order Monte Carlo results from our program (run for fixed  $v$ ) correspondingly. The statistical error is below the size of the dots and squares. Squares at low  $z$  are omitted in order not to obscure the picture. (They fall there at a constant distance below dots.) The solid curve corresponds to the second order analytical result with the "exponentiation" as given by formula (6.1) and the dashed curve represents the first order analytical "exponentiated" result [3]. This plot is almost  $\sqrt{s}$  independent. We have used again  $\sqrt{s} = M_Z = 92\text{GeV}$  and  $\epsilon = 10^{-6}$ .

**TPJU-15/88** pow. w IFUJ

zam. 20/88, 270 egz.

**Fig. 1**

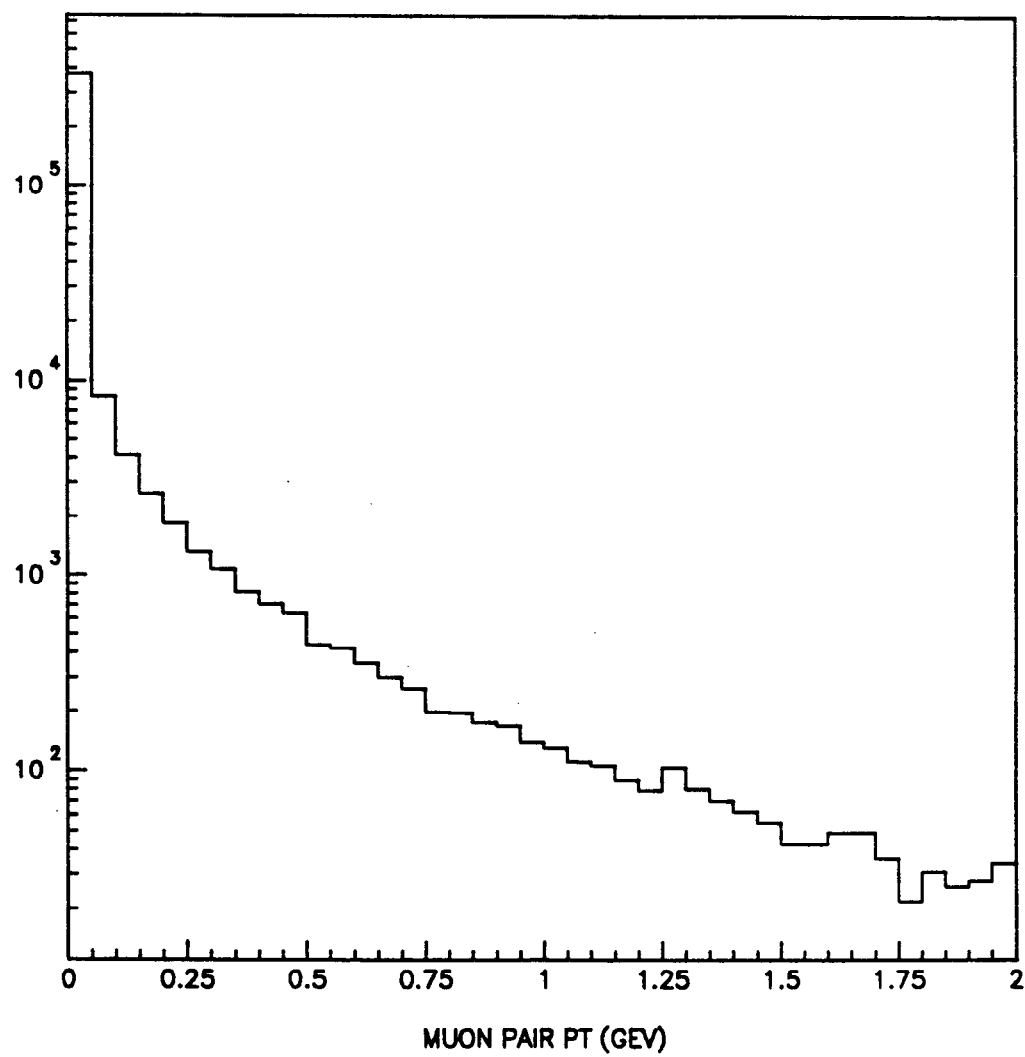


**Fig. 2**

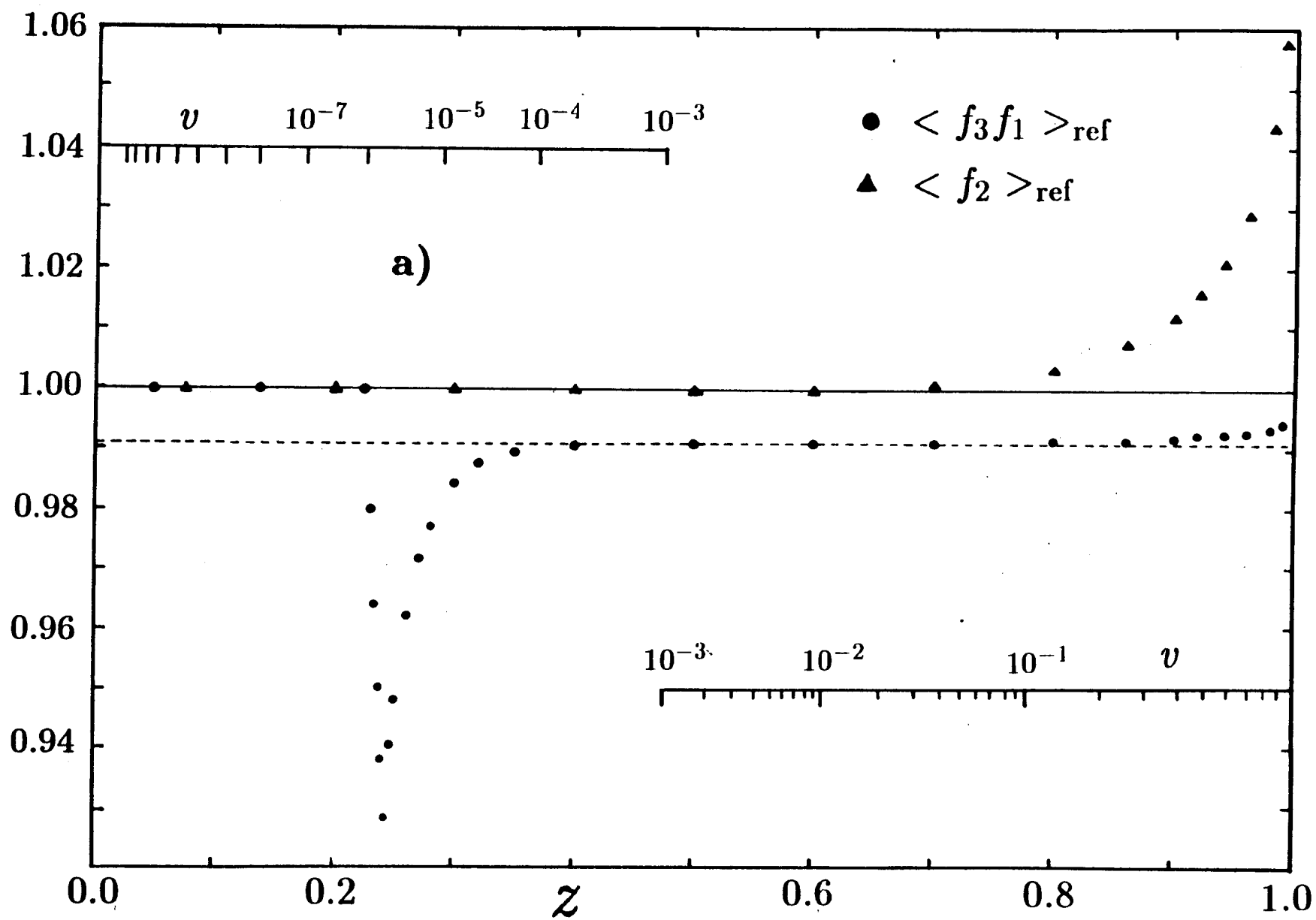


Fig. 3a

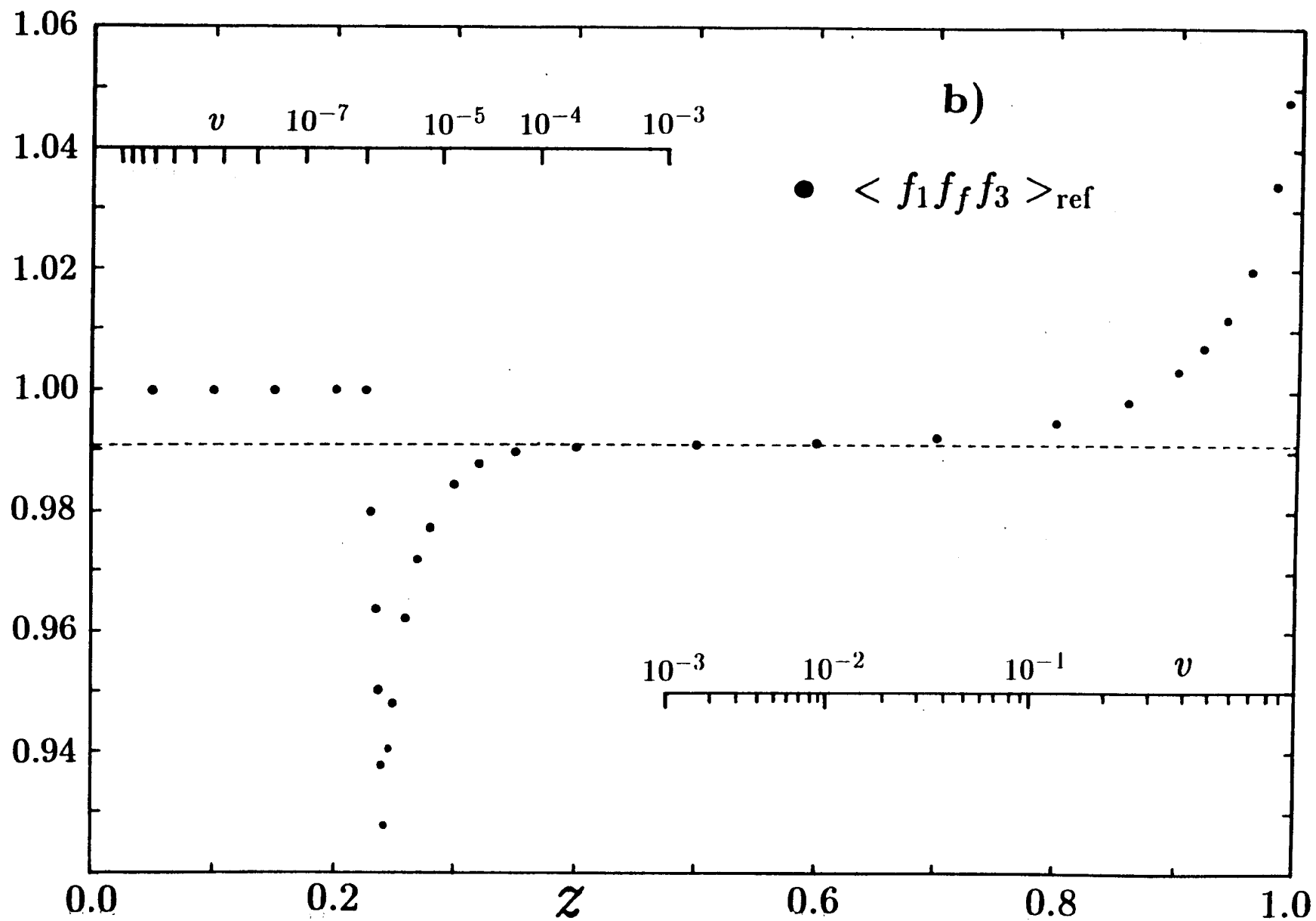


Fig. 3b

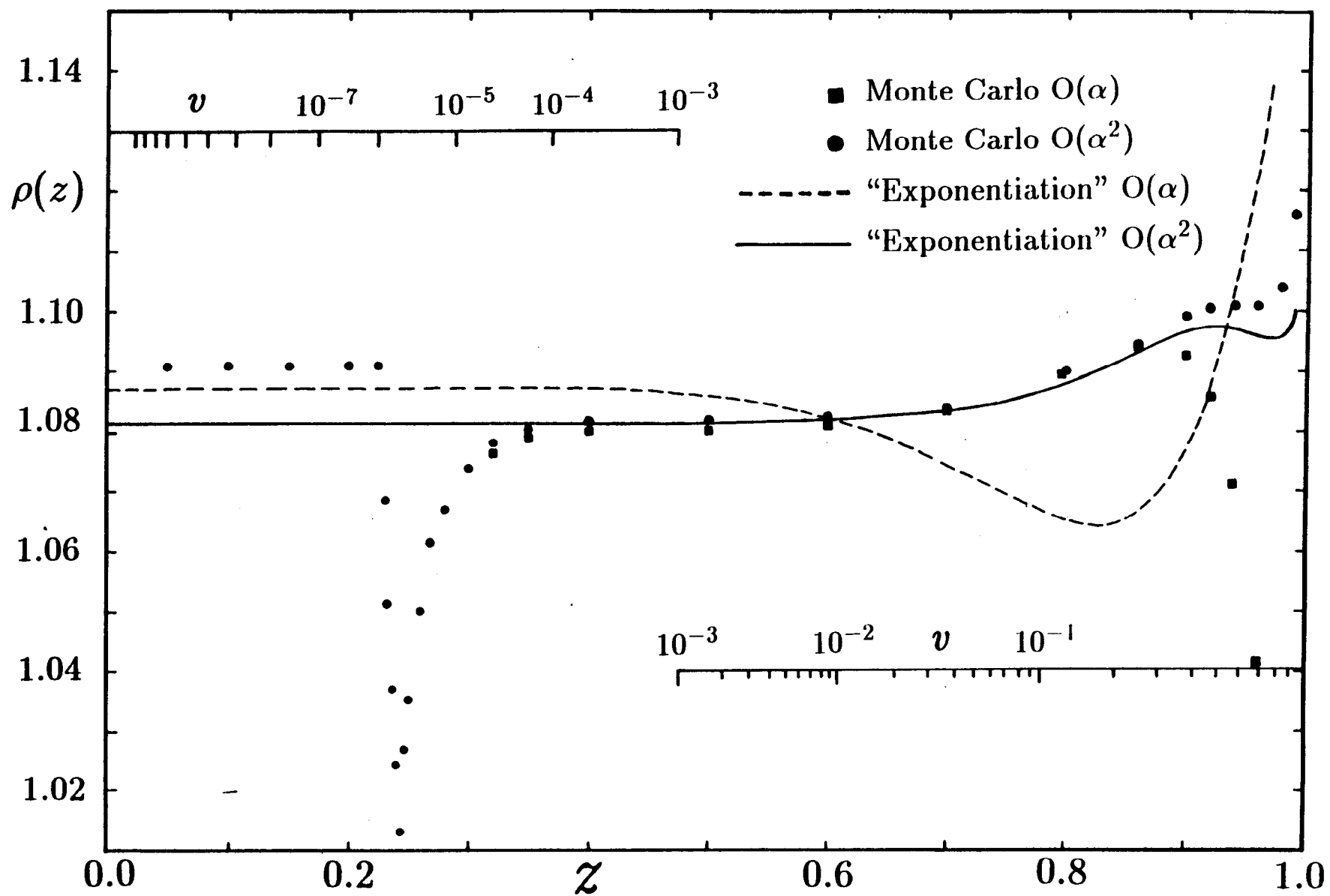


Fig. 4

# EXCERPTS FROM THE OUTPUT

```

*****
*                                     ( YFS VERSION 2.2  NOVEMBER 88 )                                     *
*                                     EXPAND  INPUT  PARAMETERS                                         *
*      92.000000000    CMSENE *  CMS ENERGY                                                         *
*      3               KEYRAD *  RADIATION SWITCH                                                       *
*      0.105000000    AMFIN *  FINAL FERMION MASS                                                       *
*      92.000000000    AMAZ *  MASS OF Z0                                                             *
*      2.453460000    GAMMZ *  WIDTH OF Z0                                                            *
*      0.228818000    SINW2 *  SIN(THETW)**2                                                           *
*      0.000001000    VVMIN *  MINIMUM VALUE OF V-PARAMETER                                           *
*      0.800000000    VVMAX *  MAXIMUM VALUE OF V-PARAMETER                                           *
*****

=====DUMPS=====
QF1  17.45970990557074 23.44740398671347-35.41734494924665 45.92408487881668
QF2 -17.47243176468074-23.44084321242244 35.50152653410081 45.99052525827749
PHO  0.01272185911000 -0.00656077429103 -0.08418158485416 0.08538986290580
SUM  0.00000000000000 0.00000000000000 0.00000000000000 91.99999999999997

=====DUMPS=====
QF1  13.62446124335595 22.25003776671934-37.88412045420546 45.99899708016354
QF2 -13.62446320902179-22.25002815088870 37.88522260179111 45.99990072855150
PHO  0.00000196566584 -0.00000961583065 -0.00110214758565 0.00110219128494
SUM  0.00000000000000 0.00000000000000 0.00000000000000 91.99999999999998

=====DUMPS=====
QF1 -12.04727357422227 -4.99932546917594 43.12337263409677 45.05292829615043
QF2  12.04799691161893  4.99874862853679-44.09028678007265 45.97940985683405
PHO  0.00001610246097  0.00115357194465  0.96669904757151  0.96669973599002
PHO -0.00073943985763 -0.00057673130550  0.00021509840438  0.00096211102549
SUM  0.00000000000000  0.00000000000000  0.00000000000000  91.99999999999998

=====DUMPS=====
QF1 -13.93314269222713 43.18265952721784  7.11399734053975 45.92923396146279
QF2  13.94316472836349-43.18680468544265 -6.95549770228890 45.91189295669911
PHO -0.01002264579176  0.00414432763129 -0.15730563366891  0.15767907681161
PHO  0.00000060965540  0.00000083059352 -0.00119400458194  0.00119400502647
SUM  0.00000000000000  0.00000000000000  0.00000000000000  91.99999999999998

=====DUMPS=====
QF1 -45.80956016230473  2.00688772322648 -3.66682074862488 46.00000000000000
QF2  45.80956016230473 -2.00688772322648  3.66682074862488 46.00000000000000
SUM  0.00000000000000  0.00000000000000  0.00000000000000 92.00000000000000

```

```

*****
*                                     KARLUD FINAL REPORT                                     *
*                                     WINDOW A                                             *
*      1161134      NEVTOT * NO OF EVENTS - TOTAL                                     A0 *
*                   0      NEVNEG * NO OF EVENTS WITH WT<0                           A1 *
*                   0      NEVOVE * NO OF EVENTS WITH WT>1                           A2 *
*      128.427451914  XCVESK * CRUDE XSEC. FROM VESKO                               A3 *
*      128.427405776  XCGAUS * CRUDE XSEC. FROM GAUSS INTEGR.                       A4 *
*                   0.000000359  XCVESK/XCGAUS-1                                   A5 *
*                   0.000048788  ERELAT * RELATIVE ERROR (VESKO)                     A6 *
*                   0.943193797  WTKARL * AVERAGE TOTAL WEIGHT                       A7 *
*                   0.000171572  ERKARL * DISP/AVER. FOR WTKARL                     A8 *
*                   121.131932488  XSKARL=AVER(WT1*WT2*WT3)*CRUDE (SIGMAPRIM) A9 *
*****

*****
*                                     KARLUD FINAL REPORT CONT.                           *
*                                     WINDOW B                                             *
*      0.000092282    AVERAGE(WF1)-1,      WF1=MASS WEIGHT                           B0 *
*      0.000145674    ERROR STAT.                                                    B1 *
*      1.000156608    AVERAGE(WF2),        WF2=FIRST DIL. WT                        B2 *
*      0.000003035    ERROR STAT.                                                    B3 *
*      0.990304695    AVERAGE(WF3)         WF3=SECOND DIL. WT                      B4 *
*      0.000123166    AVERAGE(WF3) -YGAMF(BETI2)                                    B5 *
*      0.000094124    ERROR STAT.                                                    B6 *
*      0.991008354    AVERAGE(WF1*WF3)                                             B7 *
*      0.000054395    AVERAGE(WF1*WF3)-YGAMF(BETI)                                B8 *
*      0.000173002    ERROR STAT.                                                    B9 *
*****

*****
*                                     KARLUD FINAL REPORT CONT.                           *
*                                     WINDOW C                                             *
*      0.107785610    BETI= 2*ALFA/PI*(LOG(S/MEL**2)-1)                            C0 *
*      0.990444794    GAMFAP= 1-PI**2*BETI**2/12                                    C1 *
*      0.990953959    GAMFAC=EXP(-CEULER*BETI)/GAMMA(1+BETI)                        C2 *
*      0.990181530    GAMFA2=EXP(-CEULER*BETI2)/GAMMA(1+BETI2)                      C3 *
*      0.991154034    AVERAGE(WF1*WF2*WF3)                                         C4 *
*      0.000200075    AVERAGE(WF1*WF2*WF3)-YGAMF(BETI)                            C5 *
*      0.000173032    ERROR STAT.                                                    C6 *
*      122.217810423  XREFER= REFERENCE CSECTION BREMKF(10)                        C7 *
*                                     CROSS-CHECKS                                       *
*      0.000039159    XREFER*AVER(WF1*WF1*WF3)/XSKARL-1D0                          C8 *
*      0.000030132    XCRUDE*AVER(WTR)/XREFER-1D0                                  C9 *
*****

```



```

*****
*                                     EXPAND OUTPUT - WINDOW A                                     *
*          92.000000000          CMSENE * CMS ENERGY                                     *
*                                     TOTAL XSEC FROM MONTE CARLO                             *
*          131.526546987          XSMC * IN R UNITS                                     A0 *
*          0.037331985          * ABSOLUTE ERROR                                     A1 *
*          1.349696092          XSMCNB * IN NANOBARNS                                     A2 *
*          0.000383093          * ABSOLUTE ERROR                                     A3 *
*          0.000283836          EREL * RELATIVE ERROR                                     A4 *
*          1161134          NEVTOT * NO OF EVENTS - TOTAL                             A5 *
*          396985          NEVACC * ACCEPTED                                     A6 *
*          0          NEVNEG * WITH NEGATIVE WEIGHT                                     A7 *
*          0          NEVOVE * WITH WT > WTMAX                                     A8 *
*          1.846459055          XBORN * BORN IN NANOBARNS                             A9 *
*****

```

```

*****
*                                     EXPAND OUTPUT - WINDOW B                                     *
*                                     XSECTIONS IN R-UNITS                             *
*          132.164227929          XS20 * BETA0 CROSS SECTION                             B0 *
*          0.000283583          EREL20 - RELATIVE ERROR                             *
*          131.517912565          XS21 * BETA0+BETA1 XSECTION                             B1 *
*          0.000283932          EREL21 - RELATIVE ERROR                             *
*          131.526546987          XS22 * BETA0+BETA1+BETA2 XSECT                             B2 *
*          0.000283836          EREL22 - RELATIVE ERROR                             *
*          -0.004913954          * RELAT. CONTRIB. FROM BETA1                             B3 *
*          -0.000023550          - AND ITS ERROR                                     *
*          0.000065648          * RELAT. CONTRIB. FROM BETA2                             B4 *
*          0.000002463          - AND ITS ERROR                                     *
*          131.334533181          XS25 * BETA0+BETA1 ORDER(1) ONLY                             B5 *
*          0.000283918          EREL25 - RELATIVE ERROR                             *
*          -0.001459886          XS25/XS22-1 = ORDER(1)/ORDER(2)-1                             B6 *
*          0.000401463          - RELATIVE ERROR                                     *
*****

```

```

*****
*                                     EXPAND OUTPUT - WINDOW C                                     *
*          131.526546987          XSMC * MONTE CARLO CROSS SECTION                             C0 *
*          0.000283836          RELATIVE ERROR                                     C1 *
*          132.035619586          XREF2 * FIRST ORDER TYPE-2                             C2 *
*          -0.003855570          XSMC/XSKF2-1                                     C3 *
*          131.363550846          XREF3 * FIRST ORDER TYPE-3                             C4 *
*          0.001240802          XSMC/XSKF3-1                                     C5 *
*          131.512547019          XREF4 * SECOND ORDER TYPE-4                             C6 *
*          0.000106453          XSMC/XSKF4-1                                     C7 *
*          131.556613969          XREF5 * SECOND ORDER TYPE-5                             C8 *
*          -0.000228548          XSMC/XSKF5-1                                     C9 *
*****

```